This article has not been copyedited and formatted. The final version may differ from this version.
DMD Fast Forward. Published on February 22, 2012 as doi:10.1124/dmd.111.043117

DMD # 043117

Optimized Assays for Human UDP-Glucuronosyltransferase (UGT) Activities: Altered Alamethicin Concentration and Utility to Screen for UGT Inhibitors

Robert L. Walsky, Jonathan N. Bauman, Karine Bourcier, Georgina Giddens, Kimberly Lapham, Andre Negahban, Tim F. Ryder, R. Scott Obach, Ruth Hyland, and Theunis C. Goosen

Department of Pharmacokinetics, Dynamics, and Metabolism, Pfizer Inc., Groton, Connecticut (RLW, JNB, KL, AN, TFR, RSO, TCG), and Sandwich, Kent, United Kingdom (KB, GG, RH)

DMD # 043117

Running Title: UGT Inhibition Assays

Address for Correspondence:

Dr. Theunis C. Goosen, Department of Pharmacokinetics, Dynamics, and Metabolism, Pfizer Worldwide Research and Development, Eastern Point Road, MS 8220-3525, Groton, CT 06340

Phone: +1 (860) 686-9380, Fax: +1 (860) 686-7617, Email: theunis.goosen@pfizer.com

Number of Text Pages: 42

Number of Tables: 6

Number of Figures: 6 (plus two supplemental figures)

Number of References: 63

Number of Words:

Abstract: 247

Introduction: 749

Discussion: 1447

Abbreviations: AZT, 3′-azido-3′-deoxythymidine or zidovudine; AZT-G: AZT-5′-glucuronide; BSA, bovine serum albumin; CL_{int}, intrinsic clearance; CL_{max}, maximal clearance; CL_H, hepatic clearance; CI, 95% confidence interval; DDI, drug-drug interaction; DMSO, dimethyl sulfoxide; ES, β-estradiol; ES3-G, β-estradiol-3-glucuronide; HMBC, heteronuclear multiple bond coherence; HLM, human liver microsome; HPLC, high pressure liquid chromatography; 5HTOL, 5-hydroxytryptophol; 5HTOL-G, 5-hydroxytryptophol-*O*-glucuronide; IC_{50}, apparent 50% inhibition concentration; IS, internal standard; LC-MS/MS, liquid chromatography equipped with tandem mass spectrometry; NCE, new chemical entity; PRO, propofol; PRO-G, propofol-*O*-glucuronide; rUGT, recombinant UGT; TFP, trifluoperazine; TFP-G, trifluoperazine-*N*-glucuronide; UGT, UDP-glucuronosyltransferase; UDPGA, UDP-glucuronic acid.

DMD Fast Forward. Published on February 22, 2012 as DOI: 10.1124/dmd.111.043117
This article has not been copyedited and formatted. The final version may differ from this version.

ABSTRACT

The measurement of the effect of new chemical entities on human UDP-glucuronosyltransferase (UGT) marker activities using *in vitro* experimentation represents an important experimental approach in drug development to guide clinical drug interaction study design or support claims that no *in vivo* interaction will occur. Selective high-performance liquid chromatography-tandem mass spectrometry functional assays of authentic glucuronides for five major hepatic UGT probe substrates were developed: β-estradiol-3-glucuronide (UGT1A1), trifluoperazine-*N*-glucuronide (UGT1A4), 5-hydroxytryptophol-*O*-glucuronide (UGT1A6), propofol-*O*-glucuronide (UGT1A9), and zidovudine-5′-glucuronide (UGT2B7). High analytical sensitivity permitted characterization of enzyme kinetic parameters at low human liver microsomal and recombinant UGT protein concentration (0.025 mg/ml), which led to a new recommended optimal universal alamethicin activation concentration of 10 μg/ml for microsomes. Alamethicin was not required for recombinant UGT incubations. Apparent enzyme kinetic parameters, particularly for UGT1A1 and UGT1A4, were impacted by nonspecific binding. Unbound intrinsic clearance for UGTs 1A9 and 2B7 increased significantly following addition of 2% bovine serum albumin, with minimal changes for UGT1A1, UGT1A4, and UGT1A6. Eleven potential UGT and cytochrome P450 inhibitors were evaluated as UGT inhibitors, resulting in observation of nonselective UGT inhibition by chrysin, mefenamic acid, silybinin, tangeretin, ketoconazole, itraconazole, ritonavir, and verapamil. The pan-cytochrome P450 inhibitor, 1-aminobenzotriazole, minimally inhibited UGT activities and may be useful in reaction phenotyping of mixed UGT and cytochrome P450 substrates. These methods should prove useful in the routine assessments of the potential for new drug candidates to elicit pharmacokinetic drug interactions via inhibition of human UGT activities and the identification of UGT-enzyme selective chemical inhibitors.

DMD Fast Forward. Published on February 22, 2012 as DOI: 10.1124/dmd.111.043117
This article has not been copyedited and formatted. The final version may differ from this version.

Introduction

Drug-drug interactions (DDIs) due to the inhibition of UDP-glucuronosyltransferases (UGTs), both as perpetrator and victim, should be considered when developing new chemical entities (NCEs) and are of importance in drug discovery research or evaluation of patient safety by regulatory agencies (Bjornsson et al., 2003; Zhang et al., 2010). In general, the risk of significant clinical DDIs due to the inhibition of UGTs during drug co-administration is low in comparison to inhibition of cytochrome P450 (CYP) activities (Williams et al., 2004; Kiang et al., 2005). Similarly, few clinically relevant examples requiring dose adjustment for a poor UGT metabolizer genotype exist, except for clinical reports on UGT1A1 substrates (Toffoli et al., 2006; Williams et al., 2008; Court, 2010). Nevertheless, thorough evaluation throughout discovery and development of new drugs is required to inform the potential for a significant DDI liability. Accordingly, the development of reliable and robust assay conditions and analytical methods for measuring glucuronidation *in vitro*, which could be employed to obtain relative activity factors (Venkatakrishnan et al., 2000) and develop appropriate tools useful in identifying UGT-enzyme-selective chemical inhibitors are required to advance UGT reaction phenotyping techniques (Miners et al., 2010a; Parkinson et al., 2010).

UGT 1A1, 1A3, 1A4, 1A6, 1A9, 2B7, and 2B15 are considered to play a significant role in hepatic drug and xenobiotic metabolism (Miners et al., 2010a) of the nineteen human UGTs currently identified (Mackenzie et al., 2005; Miners et al., 2010b). The triad of UGT reaction phenotyping techniques are not equally advanced (Court, 2004). In particular, a limited number of UGT-selective probe substrates are available to correlate *in vitro* glucuronidation activities of the major UGTs expressed in human liver with those of drugs or NCEs in HLMs or hepatocytes, or evaluate UGT contribution in DDIs through either enzyme inhibition or induction (Court, 2005; Miners et al., 2010a). During the course of these studies, selective LC-MS/MS functional assays of authentic glucuronides for five major hepatic UGT probe substrates (Figure 1) were developed. Selective UGT1A1 substates include bilirubin and etoposide, but due to challenging substrate assays, ES is most widely used to characterize UGT1A1 kinetics with the understanding that other hepatic UGTs (e.g. UGT1A3) may contribute to ES3-G

DMD Fast Forward. Published on February 22, 2012 as DOI: 10.1124/dmd.111.043117
This article has not been copyedited and formatted. The final version may differ from this version.

formation (Lepine et al., 2004; Itäaho et al., 2008). TFP is selective for measurement of UGT1A4 activity (Uchaipichat et al., 2006a) and other potentially selective substrates have been characterized (e.g. 1-hydroxymidazolam) (Miners et al., 2010a). In addition to serotonin (5-hydroxytryptamine), the metabolite 5HTOL has been identified with LC/UV quantification as a marker substrate for UGT1A6 (Krishnaswamy et al., 2004). Literature reports have shown convincing evidence of PRO selectivity for UGT1A9 activity (Soars et al., 2004; Court, 2005) and AZT is an established UGT2B7 probe substrate (Court et al., 2003).

Several experimental variables impact *in vitro* UGT enzyme activity and ultimately intrinsic clearance (CL_{int}) estimates, including buffer type, pH, and ionic strength, latency, organic solvent, glucuronide stability, atypical kinetics, and the albumin effect (Easterbrook et al., 2001; Fisher et al., 2001; Boase and Miners, 2002; Soars et al., 2003; Uchaipichat et al., 2004; Engtrakul et al., 2005; Rowland et al., 2007; Rowland et al., 2008). The latter resulting from long-chain unsaturated fatty acids being released from membranes during the course of an incubation and acting as potent inhibitors of UGT1A9, UGT2B7, and microsomal glucuronidation activity, resulting in overestimation of the K_m value (Tsoutsikos et al., 2004; Rowland et al., 2007; Rowland et al., 2008). Inhibitory fatty acids are sequestered by addition of BSA and altered incubation conditions, in the presence and absence of BSA, should be evaluated to select appropriate substrate concentrations ($\leq K_m$) when employed in an inhibitor screening assay. The objectives of the studies described herein are to develop improved analytical methods (Donato et al., 2010) for measuring the *in vitro* activities of five major human UGT enzymes employing authentic analytical glucuronide standards (Figure 1) analogous to those for CYP (Walsky and Obach, 2004). In addition, to evaluate these methods in high-throughput UGT inhibitor screening of several potential inhibitors of these enzymes. Various attributes of incubation conditions frequently used to measure UGT activities (e.g. albumin, buffer, saccharolactone, and alamethicin) were explored in order to define optimal conditions for each enzyme at low protein concentration. In the course of these studies, the more precise identification of the glucuronide metabolite of 5-hydroxytryptophol was made to facilitate the development of the assay for UGT1A6. The findings are described in this report, and these

assay methods should be of use to investigators engaged in research on these enzymes and the xenobiotics they metabolize.

DMD Fast Forward. Published on February 22, 2012 as DOI: 10.1124/dmd.111.043117
This article has not been copyedited and formatted. The final version may differ from this version.

Materials and Methods

Materials. Substrates, metabolite standards, internal standards, and other materials were from the following sources: AZT-5′-glucuronide, [$^{13}C_6$]AZT-5′-glucuronide, 5-hydroxytryptophol, propofol-*O*-glucuronide, trifluoperazine-*N*-glucuronide, [D_3]trifluoperazine-*N*-glucuronide (Cerilliant, Austin, TX); magnesium chloride, potassium phosphate, Tris (base), Tris-HCl, (J.T.Baker, Phillipsburg, NJ); ammonium formate, formic acid, (Fluka, Buchs AG, Switzerland); alamethicin, AZT, bovine serum albumin (crude BSA product no. A7906), diclofenac, β-estradiol, β-estradiol-3-glucuronide, β-estradiol-17-glucuronide, propofol, and D-saccharic acid 1,4-lactone (saccharolactone), uridine-diphosphate-glucuronic acid trisodium salt (UDPGA) (Sigma Chemical Co., St. Louis, MO); 1-naphthyl-glucuronide (Sequoia Research Products, Ltd., Pangbourne, UK). Inhibitors were from Sigma Chemical Co. (St. Louis, MO) or Sequoia Research Products (Pangbourne, UK). Pure ("100%") stable-labeled dimethylsulfoxide (DMSO-d_6) and methanol-d_4 were from Cambridge Isotope Laboratories, Inc. (Andover, MA). 5-Hydroxytryptophol-*O*-glucuronide was obtained by biosynthesis as detailed below. Other reagents and solvents used were from standard suppliers and were of reagent or HPLC grade with all purities as defined by the manufacturer.

Human liver microsomes were prepared from a mixed gender pool of 50 donors provided by BD Biosciences (Woburn, MA). Recombinant UGT1A1, UGT1A4, UGT1A6, UGT1A9, and UGT2B7 Supersomes™ were heterologously expressed from human cDNA in a baculovirus expression system; protein concentrations and initial activity assessments were provided by the manufacturer (BD Biosciences, Woburn, MA).

General UGT Assay Incubation Conditions. Specific aspects of the incubation condition for each assay are defined in Table 1. In general, for the final optimized method, a premix containing HLM or expressed UGT enzyme (0.025 mg/ml) were mixed with 100 mM Tris-HCl buffer (pH 7.5 at 37°C), $MgCl_2$ (5 mM), substrate, alamethicin (10 μg/ml), with or without 2% BSA. The premix was placed on ice for 15 minutes to allow alamethicin pore formation to occur and then aliquots of this mixture (0.09

DMD Fast Forward. Published on February 22, 2012 as DOI: 10.1124/dmd.111.043117
This article has not been copyedited and formatted. The final version may differ from this version.

ml) were delivered to each well of a 96-well polypropylene PCR plate maintained at 37°C containing the inhibitor or control solvent (DMSO), as applicable. Final solvent concentrations were 1% (v/v) or less. Incubations were commenced with the addition of UDPGA (5 mM) to a final incubation volume of 0.1 ml and incubated at 37°C for the period defined in Table 1. Incubations were typically terminated by addition of acidified organic solvent (acetonitrile) containing internal standard. The terminated incubation mixtures were centrifuged and either directly injected, evaporated under nitrogen and reconstituted, or filtered before transferring into a receiver 96-well micro-titer plate for LC-MS/MS analysis as described below.

Optimization of UGT Assay Incubation Conditions. Linearity of product formation with respect to time and protein concentration were conducted with HLM and rUGT for each assay. Multiple time course experiments were conducted to evaluate the effects of: 100 mM Tris-HCl versus 100 mM phosphate buffers (pH 7.5), $MgCl_2$ concentration (0, 1, 5, 10 mM), and use of 5 mM saccharolactone. Incubations (1.0 ml) were conducted as described above at four HLM or rUGT protein concentrations (0.01, 0.025, 0.05, 0.1 mg/ml) for each specific UGT assay at substrate concentrations approximating S_{50} or K_m (Table 2). Aliquots (0.1 ml, N=2) were typically collected over a 90-min time course, terminated, and analyzed for metabolite formation as described below.

Alamethicin concentrations were optimized using pooled HLM and rUGT for UGT1A1, UGT1A4, and UGT2B7 since initial incubations for UGT2B7 performed with published alamethicin concentrations (50 µg/mg protein) shown optimal for pore-formation (Fisher et al., 2000) were not linear. Alamethicin, dissolved in MeOH/water (50/50) as a 100X stock, was evaluated with four pooled HLM or rUGT protein concentrations (0.01, 0.05, 0.2, 0.5 mg/ml), each assessed without and with alamethicin (1-25 µg/ml, N=3) pretreatment at the appropriate substrate S_{50} or K_m.

Determination of Nonspecific Protein Binding. The fraction of unbound substrate in incubation matrices ($f_{u,inc}$) was determined by equilibrium dialysis using the rapid equilibrium dialysis (RED) method (Waters et al., 2008). Substrates were spiked into the human liver microsomal sample (0.025 mg/ml, with and without 2% BSA; 2.0 ml incubation volume) at a concentration close to the K_m or

DMD Fast Forward. Published on February 22, 2012 as DOI: 10.1124/dmd.111.043117
This article has not been copyedited and formatted. The final version may differ from this version.

S_{50}, dialyzed against incubation mixture on a shaker (450 rpm) within a humidified CO_2 (5%) incubator at 37°C in the absence of protein (HLM or BSA) for 4 hours. Aliquots (0.22 ml) were removed to assess recovery and at the end of the incubation, protein precipitated with acetonitrile (0.18 ml containing 5% DMSO and IS) and analyzed by LC/MS/MS as described below.

UGT Enzyme Kinetic and Inhibition Experiments. Substrate saturation experiments were conducted to generate rate data for determining the appropriate enzyme kinetic fit (see *Data Analysis*) and the apparent substrate K_m and V_{max} values were calculated for each assay in pooled HLMs and rUGT enzyme. The experiments were performed using at least eight substrate concentrations spanning the anticipated K_m (N=3) with and without addition of 2% BSA (w/v). Incubations were typically performed in a polypropylene 96-well PCR plate which was incubated using a thermostatically controlled heater block, or a shaking water bath, at 37°C as described above. Briefly, aliquots (0.09 ml) of pooled HLM, or rUGT enzyme premix were prewarmed at 37°C for 5 minutes prior to initiation with 0.01 ml of UDPGA (5 mM). The samples were incubated for the times indicated in Table 1, terminated by the addition of an internal standard as described for each assay and analyzed to quantify the specific glucuronide products by LC-MS/MS as detailed below.

β-Estradiol-3-Glucuronide (UGT1A1) Assay. Unless otherwise indicated, β-estradiol (ES) (3-1000 μM final) was incubated as described under *General UGT Assay Incubation Conditions*. Stock solutions of ES (100 mM), β-estradiol-3-glucuronide (ES3-G 1 mM), and α-naphthylglucuronide (0.5 mM), as internal standard, were prepared in DMSO. Reactions (0.1 ml) were terminated at the indicated times (Table 1) by addition of 0.05 ml of 47/50/3 acetonitrile/water/formic acid containing α-naphthylglucuronide (5 μM final), were centrifuged at 500*g* for 10 min and the supernatant transferred to 96-well plates for LC-MS/MS analysis as below. ES3-G standard curve samples (0.02-2.5 μM final) were serially diluted (1:100) in incubation matrix and treated identically to samples. The LC-MS/MS method employed a binary gradient using water/0.1% formic acid (mobile phase A) and acetonitrile/0.1% formic acid (mobile phase B). A mobile phase composition of 29% B was held for 2.0 minutes, then

DMD Fast Forward. Published on February 22, 2012 as DOI: 10.1124/dmd.111.043117
This article has not been copyedited and formatted. The final version may differ from this version.

ramped to 90% B over 2.1 minutes, returned to 29% B over 0.1 minutes and held. ES and ES3-G were analytically separated on a Phenomenex Gemini 5µ C_{18} 2.0 x 50 mm (Phenomex, Torrance, CA) column. Under these HPLC conditions ES3-G, β-estradiol-17-glucuronide, and the IS (α-naphthylglucuronide) had elution times of 1.3, 1.9, and 1.1 minutes, respectively.

Trifluoperazine *N*-Glucuronide (UGT1A4) Assay. Unless otherwise indicated, trifluoperazine (TFP) (1-550 µM final) was incubated as described under *General UGT Assay Incubation Conditions*. Stock solutions of TFP (55 mM) were prepared in DMSO. TFP-G (0.858 mM), and [D_3] TFP-G (0.03 mM), as internal standard, were prepared in water/acetonitrile (50/50). Reactions (0.1 ml) were terminated at the indicated time (Table 1) by addition of 0.01 ml of 17/80/3 acetonitrile/water/formic acid containing [D_3]trifluoperazine-*N*-glucuronide ([D_3]TFP-G, 3 µM final) as IS, were centrifuged at 500*g* for 10 min and the supernatant transferred to 96-well plates for LC-MS/MS analysis as below. TFP-G standard curve samples (0.017-8.6 µM final) were serially diluted (1:100) in incubation mixture and treated identically to samples. The LC-MS/MS method employed a binary gradient using water/0.1% formic acid (mobile phase A) and acetonitrile/0.1% formic acid (mobile phase B). A mobile phase composition of 10% B was held for 0.1 minutes, then ramped to 80% B over 1.9 minutes (2.0 minutes total), returned to 10% B over 0.1 minutes and held (3.0 min total). Analytes were separated on a Phenomenex Synergi max-RP 4µ 2 x 30 mm (Phenomex, Torrance, CA) column. Under these HPLC conditions, TFP-G and the IS ([D_3]TFP-G) had elution times of 1.2 and 1.1 minutes, respectively.

5-Hydroxytryptophol-*O*-Glucuronide (UGT1A6) Assay. Unless otherwise indicated, 5-hydroxytryptophol (5HTOL) (20-10,000 µM final) was incubated as described under *General UGT Assay Incubation Conditions*. Stock solutions of 5HTOL, 5-hydroxytryptophol-*O*-glucuronide (5HTOL-G) (6.6 mM), and diclofenac (0.32 µM) were prepared in water, DMSO-d_6, and acetonitrile, respectively. 5HTOL-G concentrations were determined by quantitative NMR employing the artificial signal insertion for calculation of concentration observed (aSICCO) method described by Walker et al., 2011. Reactions (0.1 ml) were terminated at the indicated times (Table 1) by the addition of 0.3 ml acetonitrile containing

DMD Fast Forward. Published on February 22, 2012 as DOI: 10.1124/dmd.111.043117
This article has not been copyedited and formatted. The final version may differ from this version.

diclofenac (0.24 μM) as an internal standard, were centrifuged at 500*g* for 10 min and the supernatant (0.3 ml) transferred to 96-well plates, evaporated to dryness under nitrogen at 40°C, and reconstituted in 5/95 acetonitrile/water (0.1 ml) containing 0.1% formic acid for LC-MS/MS analysis as below. 5HTOL-G standard curve samples (0.01-20 μM) were serially diluted (1:10) in incubation matrix and treated identically to samples. The LC-MS/MS method employed a binary gradient with 95/5 water/acetonitrile containing 0.1% formic acid (mobile phase A) and 95/5 acetonitrile/water containing 0.1% formic acid (mobile phase B). A mobile phase composition of 20% B was ramped to 95% B over 1.6 minutes and maintained for 0.2 min (1.8 min total), returned to 10% B over 0.1 minutes and held (2.5 min total). Analytes were separated on a Waters XTerra MS 3.5μ C_{18} 2.1 x 100 mm (Waters, Milford, MA) column. Under these conditions, 5HTOL-G and the IS (diclofenac) had elution times of 1.4 and 1.1 minutes, respectively.

Propofol-*O*-Glucuronide (UGT1A9) Assay. Unless otherwise indicated, propofol (PRO) (1-1000 μM final) was incubated as described under *General UGT Assay Incubation Conditions*. Stock solutions of PRO (100 mM) and PRO-G (1.1 mM) were prepared in methanol/water (50/50) and diclofenac (0.629 μM), as internal standard, in acetonitrile. Reactions (0.2 ml) were terminated at the indicated times (Table 1) by the addition of 0.4 ml of acetonitrile containing 0.63 μM diclofenac (0.42 μM final) as IS, were centrifuged at 500*g* for 10 min and the supernatant transferred to 96-well plates for LC-MS/MS analysis as below. PRO-G standard curve samples (0.14-28 μM final) were serially diluted (1:40) in incubation matrix and treated identically to samples. The LC-MS/MS method employed a binary gradient using 95/5 water/acetonitrile containing 0.01% formic acid (mobile phase A) and acetonitrile/0.01% formic acid (mobile phase B). A mobile phase composition of 90% B was held for 1.2 minutes, then ramped to 97% B over 1.2 minutes (4.2 minutes total), returned to 90% B over 0.1 minutes and held (5.0 min total). Analytes were separated with a Waters SunFire 3.5μ C_{18} 2.1 x 30 mm (Waters, Milford, MA) column. Under these HPLC conditions, PRO-G and the IS (diclofenac) had elution times of 1.3 and 1.1 minutes, respectively. PRO quantitation for nonspecific protein binding were performed on

DMD Fast Forward. Published on February 22, 2012 as DOI: 10.1124/dmd.111.043117
This article has not been copyedited and formatted. The final version may differ from this version.

an AB Sciex API5500 QTrap mass spectrometer equipped with an electrospray source (ESI) in negative detection mode (AB Sciex LLC, Foster City, CA), two Shimadzu LC-20AD pumps, a CBM20A controller, and DGU-20A solvent degasser (Shimadzu, Columbia, MD), a LEAP CTC HTS PAL autosampler (CTC Analytics, Carrboro, NC), and a Valco 2-position switching valve (Huston, TX). Separation was on a Kinetex 2.6µ C_{18} 50 x 2 mm column and the LC-MS/MS method employed a binary gradient using water/0.01% formic acid (mobile phase A) and acetonitrile (mobile phase B). A mobile phase composition of 5% B was held for 0.3 minutes, then ramped to 95% B over 2 minutes, held at 95% B for 0.3 min, returned to 5% B over 0.1 minutes and held (3.0 min total).

AZT-5′-Glucuronide (UGT2B7) Assay. Unless otherwise indicated, AZT (180-4500 µM final) was incubated as described under *General UGT Assay Incubation Conditions*. Stock solutions of AZT (1100 mM), AZT-G (0.5 mM), and [$^{13}C_6$] AZT-G (0.5 mM), as internal standard, were prepared in acetonitrile/water (50/50). Reactions (0.1 ml) were terminated at the indicated times (Table 1) by the addition of 0.01 ml of 5/92/3 acetonitrile/water/formic acid containing 10 µM [$^{13}C_6$]AZT-G (1 µM final) as IS, filtered on a Millipore Multiscreen-HA 0.45 µm mixed cellulose ester 96-well membrane vacuum filtration module and the filtrate transferred to 96-well plates for LC-MS/MS analysis as below. AZT-G standard curve samples (0.05-5 µM final) were serially diluted (1:100) in incubation matrix and treated identically to samples. The LC-MS/MS method employed a binary gradient using 5 mM ammonium formate/0.05% formic acid (mobile phase A) and 95/5 acetonitrile/methanol containing 0.05% formic acid (mobile phase B). A mobile phase composition of 2% B was held for 0.5 minutes, then ramped to 35% B over 2.1 minutes (2.6 minutes total), returned to 2% B over 0.1 minutes and held (4.0 min). Analytes were separated on a Phenomenex Luna 5µ $C_{18(2)}$ 3.0 x 30 mm (Phenomex, Torrance, CA) column. Under these HPLC conditions, AZT-G and the IS, [$^{13}C_6$]AZT-G, had elution times of 2.0 minutes.

UGT Inhibition Assays. In experiments where inhibition of glucuronide formation was investigated (Table 3), 50 µM and 500 µM inhibitor (final concentration) in DMSO (or solvent control)

DMD Fast Forward. Published on February 22, 2012 as DOI: 10.1124/dmd.111.043117
This article has not been copyedited and formatted. The final version may differ from this version.

were added to the 96-well plate (N=2) prior to addition of the rUGT enzyme mixture and initiated with UDPGA (5 mM) as described above. For IC_{50} determination, HLMs or rUGT were incubated with increasing inhibitor concentrations (0.1-100 µM) as described above. UGT substrate concentrations were at or below K_m; ES (10 µM or 100 µM with BSA), TFP (40 µM HLM or 67 µM with BSA; 10 µM rUGT or 140 µM with BSA), 5HTOL (350 µM), PRO (100 µM HLM, 200 µM rUGT, or 40 µM with BSA), AZT (842 µM HLM, 1080 µM rUGT, 374 µM HLM with BSA, or 596 µM rUGT with BSA).

Instrumentation. Analytical quantification was conducted by LC-MS/MS using three systems as identified in Table 1: The LC-MS/MS systems were comprised of (1) An AB Sciex LLC 4000 QTrap mass spectrometer equipped with an electrospray source (AB Sciex LLC, Foster City, CA), two Shimadzu LC-20AD pumps, a CBM20A controller, and DGU-20A solvent degasser (Shimadzu, Columbia, MD), a LEAP CTC HTS PAL autosampler using 20/80 acetonitrile/water and 80/20 acetonitrile/water (both containing 0.1% formic acid) as the wash solvents (CTC Analytics, Carrboro, NC), and a Valco 2-position switching valve (Huston, TX). (2) An AB Sciex LLC 4000 triple quadrupole mass spectrometer equipped with an electrospray source (AB Sciex LLC, Foster City, CA), two Jasco X-LCT 3080PU pumps, and a LC-NetII ADC controller (Jasco Analytical Instruments, Easton, MD), a LEAP CTC HTS PAL autosampler using 5/95 water/acetonitrile and methanol (both containing 0.1% formic acid) as the wash solvents (CTC Analytics, Carrboro, NC), and a Valco 2-position switching valve (Huston, TX). (3) A Waters Micromass Quattro Ultima triple quadrupole mass spectrometer equipped with an electrospray ionization source (Beverly, MA), two LC-10ADvp pumps with a SCL-10ADvp controller and DGU-14 solvent degasser (Shimadzu, Columbia, MD), a LEAP CTC HTS PAL autosampler with a multi-solvent peristaltic self-washing system using 5/95 water/acetonitrile and 95/5 acetonitrile/water (both containing 0.1% formic acid) as the wash solvents (CTC Analytics, Carrboro, NC), and a LabPro switching valve (Reodyne LLC, Rohnert Park, CA). In all three systems, flow was diverted from the mass spectrometer to waste for the first 0.5 min of the gradient to remove non-volatile salts.

DMD Fast Forward. Published on February 22, 2012 as DOI: 10.1124/dmd.111.043117
This article has not been copyedited and formatted. The final version may differ from this version.

Quantitative and qualitative NMR was performed using a Bruker Avance 600 MHz system controlled by TOPSPIN V2.0, equipped with a 5 mm TCI cryoprobe. Semi-preparative HPLC was performed using a Shimadzu SiL-HTC autosampler, two LC-20AD solvent pumps, an SPD-M20A diode array detector, and a FRC-10A fraction collector.

5-Hydroxytryptophol-*O*-glucuronide Isolation, Quantitation and Structural Elucidation. A pure sample of 5HTOL-G was prepared by incubating 5HTOL (200 μM) with pooled HLMs (1.0 mg/ml), UDPGA (1.0 mM), alamethicin (10 μg/ml), and $MgCl_2$ (5 mM) in 100 mM potassium phosphate buffer (pH 7.5) containing 1% BSA (4-10 ml incubations). Incubations were conducted in a shaking water bath at 37°C for 3 hours, protein precipitated by addition of acetonitrile (30 ml), supernatants combined and concentrated using an evaporative centrifuge set to 37°C. The residue was reconstituted in 10/90 acetonitrile/water (2 ml) and purified using a semi-preparative HPLC system in 5 injections (0.4 ml) using a binary gradient of 5 mM ammonium acetate/0.1% formic acid (mobile phase A) and acetonitrile (mobile phase B). A mobile phase composition of 10% B was held for 10 minutes, then ramped to 30% B over 30 minutes. Separation was performed on a Phenomenex Gemini 5μ C_{18} 10 x 250 mm (Phenomex, Torrance, CA), semi-preparative HPLC column with a flow rate of 4 ml/min. Aliquots (0.025 ml) of fractions at retention times of UV peaks believed to be the metabolite and the parent were taken for HPLC/MS/UV analysis for verification. Fractions containing 5HTOL-G were combined and concentrated to dryness using an evaporative centrifuge set to 37°C (Genevac, Valley Cottage, NY). Under these HPLC conditions, 5HTOL-G had an elution time of 13.4 minutes. The isolate was reconstituted in DMSO-d_6 (200 μL) and placed in 3 mm diameter tubes prior to NMR analysis. One-dimensional (1D)-spectra were recorded using a sweep width of 12000 Hz and a total recycle time of 7.2 s. The resulting time-averaged free induction decays were transformed using an exponential line broadening of 1.0 Hz to enhance signal to noise. All spectra were referenced using residual DMSO-d_6 (^{1}H δ=2.5 ppm and ^{13}C δ=39.5 relative to TMS, δ=0.00). Phasing, baseline correction and integration were all performed manually. If needed, the BIAS- and SLOPE-functions for the integral calculation was

DMD Fast Forward. Published on February 22, 2012 as DOI: 10.1124/dmd.111.043117
This article has not been copyedited and formatted. The final version may differ from this version.

adjusted manually. The correlation spectroscopy (COSY), multiplicity edited heteronuclear single quantum coherence (HSQC) and heteronuclear multiple bond coherence (HMBC) data were recorded using the standard pulse sequence provided by Bruker. Two-dimensional (2D) experiments were typically acquired using a 1K × 128 data with 16 dummy scans and a spectral width of 8000 Hz in the f2 dimension. The data was zero-filled to a size of 1K × 1K. A relaxation delay of 1.5 s was used between transients. Quantitation of the prepared 5HTOL-G sample was performed using the aSICCO method as previously described (Walker et al., 2011).

Data Analysis. Standard curve fitting was accomplished with AB Sciex Analyst v1.4.2 software (AB Sciex LLC, Foster City, CA) or MassLynx QuanLynx (v4.1) software (Micromass, Beverly, MA) as described above and indicated in Table 1. Data were typically fit to quadratic curves using $1/x^2$ weighting and standard curves were run for each experiment.

Substrate concentration [S] and velocity (V) data were fitted to the appropriate enzyme kinetic model by nonlinear least-squares regression analysis (Sigmaplot v12; Systat Software, Inc., Chicago, IL) to derive the apparent enzyme kinetic parameters V_{max} (maximal velocity) and K_m or S_{50} (substrate concentration at half-maximal velocity). The Michaelis-Menten model (eq. 1), the substrate inhibition model (eq. 2), and the substrate activation model (eq. 3), which incorporates the Hill coefficient (n), were used:

$$V = V_{max} \times S / (K_m + S) \quad (1)$$

$$V = V_{max} \times S / (K_m + S \times (1 + S/K_{si})) \quad (2)$$

$$V = V_{max} \times S^n / (S_{50}{}^n + S^n) \quad (3)$$

where V_{max} is the maximal velocity, K_m or S_{50} is the substrate concentration at half-maximal velocity, n is an exponent indicative of the degree of curve sigmoidicity, and K_{si} is an inhibition constant. The best fit was based on a number of criteria, including visual inspection of the data plots (Michaelis-Menten and Eadie-Hofstee), distribution of the residuals, size of the sum of the squared residuals, and the standard error of the estimates. Selection of models other than Michaelis-Menten was based on the F-test ($P <$

DMD Fast Forward. Published on February 22, 2012 as DOI: 10.1124/dmd.111.043117
This article has not been copyedited and formatted. The final version may differ from this version.

0.05) and the Akaike Information Criterion (AIC). The intrinsic clearance (CL_{int}) was calculated as the V_{max}/K_m for Michaelis-Menten and substrate inhibition kinetics and unbound intrinsic clearance ($CL_{int,u}$) was corrected for the fraction of unbound substrate in incubation ($f_{u,inc}$) as $CL_{int}/f_{u,inc}$. Since K_m and S_{50} are not equivalent, the maximum clearance (CL_{max}) is suggested as an appropriate alternate clearance parameter for substrates exhibiting substrate activation kinetics or positive cooperativity (Houston and Kenworthy, 2000; Uchaipichat et al., 2004) and was calculated from:

$$CL_{max} = \frac{V_{max}}{S_{50}} \times \frac{(n\text{-}1)}{n(n\text{-}1)^{1/n}} \quad (4)$$

IC_{50} estimates for inhibition of glucuronidation were determined by nonlinear curve fitting with Sigmaplot v12 (Systat Software, Inc., Chicago, IL) and were defined as the concentration of inhibitor required to inhibit control glucuronidation reactions by 50%.

Results

General UGT Assay Incubation Conditions. In this report, we describe optimized LC-MS/MS analytical methods for five human UDP-glucuronosyltransferase assays. While efforts were made to control any potential analytical method variability, a potentially greater source of variability resides with the incubation method. Linear conditions for each assay were established by conducting the incubations at four protein concentrations and measuring the formation of glucuronide metabolite over time. The incubation times were selected such that all reactions were linear with time (<10% substrate consumption), and the lowest protein concentration was selected such that the amount of glucuronide metabolite formed were within the dynamic range of the analytical assays (Table 1).

Optimization of UGT Incubation Conditions. Since experiments were performed at significantly lower protein concentrations (0.025 mg/ml) than typically described (0.25-2.5 mg/ml) (Fisher et al., 2000; Court, 2004; Donato et al., 2010) and considering enzyme kinetic parameters are affected by incubation conditions (Boase and Miners, 2002), a limited number of incubation conditions known to affect UGT enzyme activity were evaluated. The overall goal was to select universal incubation conditions for all five UGT assays developed and applies to the protein concentration of 0.025 mg/ml utilized in this study.

Tris versus Phosphate Buffers. Activity comparisons in human liver microsomes and recombinant UGT enzymes for UGT1A1, UGT1A4, UGT1A6, UGT1A9, and UGT2B7 substrates were conducted in 100 mM Tris-HCl (pH 7.5 at 37°C) and 100 mM potassium phosphate (pH 7.5) buffers to evaluate which provided the greatest overall glucuronide metabolite formation. Incubations in Tris buffer with HLMs showed marked increases in metabolite formation for UGT1A4 (2-fold) and UGT1A9 (~1.5-fold), while the other UGTs activities were relatively unaffected (Fig. 2). In rUGT incubations, Tris buffer resulted in increased product formation for all UGTs studied, except UGT1A6. Based on these results, a 100 mM Tris-HCl buffer was selected for all subsequent experiments.

$MgCl_2$ Concentration. To determine a common magnesium chloride concentration for use in all UGT assays, glucuronide metabolite formation was measured in HLMs and rUGT enzymes for all UGT

DMD Fast Forward. Published on February 22, 2012 as DOI: 10.1124/dmd.111.043117
This article has not been copyedited and formatted. The final version may differ from this version.

assays at 0, 1, 5, and 10 mM $MgCl_2$. The effect of $MgCl_2$ concentration on UGT activities in HLM and recombinant UGT enzymes are shown in Fig. 2. The inclusion of $MgCl_2$ in HLMs resulted in increased glucuronidation activity, ranging 2- to 4-fold for UGTs 1A1, 1A4, 1A6 and 2B7, and up to 8-fold for UGT1A9. Similar trends with more modest activation were observed in rUGTs with a 10 mM $MgCl_2$ concentration resulting in decreased activity for rUGT1A4. Based on these findings, a 5 mM $MgCl_2$ concentration was selected as general UGT incubation condition.

Inclusion of Saccharolactone. The effect of saccharolactone, an inhibitor of β-glucuronidase, was assessed at 5 mM to determine if its use was required with HLMs, and/or rUGTs for all assays developed. The fold-change in metabolite formation in the presence and absence of saccharolactone for incubations with HLMs and rUGTs are shown in Fig. 2. Saccharolactone inclusion did not significantly impact the activities of UGTs 1A1, 1A6, and 2B7 while decreases in metabolite formation were observed for UGTs 1A4 and 1A9. Based on these results, saccharolactone was excluded from the optimized UGT incubation conditions.

Alamethicin Concentration in UGT Incubations. After observing a lack of linearity between AZT-G formation and protein concentration in HLMs, which had been pretreated with alamethicin at the previously reported optimal concentration for activation (50 μg/mg HLM) (Fisher et al., 2000), the use of alamethicin at low protein concentrations was evaluated further. Four HLM protein concentrations were assessed at eight alamethicin concentrations using the optimized incubation conditions for UGT2B7 (Fig. 3), UGT1A1, and UGT1A4 (Table 2). Similar results were observed for all three enzymes studied. In general, we observed initial activation of UGT activity at a universal alamethicin concentration of 5 μg/ml and apparent maximal activation at 8.55 μg/ml. The corresponding alamethicin concentrations for 8.55 μg/ml expressed as μg/mg HLM are 855, 171, 42.8, and 17.1 μg/mg for HLM concentrations of 0.01, 0.05, 0.2 and 0.5 mg/ml HLM, respectively (Table 2). Therefore, maximal activation would be observed with 50 μg alamethicin/mg HLM only when protein concentrations exceed 0.17 mg/ml (8.55 μg/ml divided by 50 μg/mg). Accordingly, it is the alamethicin solution concentration (μg/ml) that is

DMD Fast Forward. Published on February 22, 2012 as DOI: 10.1124/dmd.111.043117
This article has not been copyedited and formatted. The final version may differ from this version.

relevant to increasing metabolite formation at the microsomal protein concentrations examined (0.01 – 0.5 mg/ml), irrespective of protein concentration in incubation. Based on these results an alamethicin concentration of 10 μg/ml is suggested as optimal for activation of UGT activity regardless of the protein concentration used; therefore, corresponding alamethicin concentrations required for activation at protein concentrations of 0.01, 0.05, 0.2 and 0.5 mg/ml are 1000, 200, 50, 20 μg/mg HLM indicating that a significantly higher alamethicin to protein ratio is required for UGT activation at low protein concentrations. As illustrated in Figure 3B, at microsomal protein concentrations below 0.2 mg/ml, no activation is realized at an alamethicin concentration of 50 μg/mg. AZT-G formation (UGT2B7) with HLMs is plotted as log alamethicin concentration in μg/ml versus metabolite formed for each protein concentration (Fig. 3A). The same data were plotted as the log of alamethicin concentration in μg/mg microsomal protein versus metabolite formed for each protein concentration to illustrate the lack of effect at low microsomal protein concentrations (Fig. 3B). An alamethicin solution concentration of at least 10 μg/ml (400 μg alamethicin/mg HLM at 0.025 mg/ml HLM) would result in optimal increases in metabolite formation in all three UGT assays and was used for all optimized incubations. Similar experiments were conducted with rUGT2B7 and showed no benefit from alamethicin addition at concentrations up to 25 μg/ml (data not shown).

Structural Interpretation of 5-hydroxytryptophol glucuronide. HPLC analysis of the isolated fraction of purified 5HTOL-G indicated a single UV peak at a retention time of 13.4 minutes using the semi-preparative HPLC system. Using an analytical column (Phenomenex HydroRP 4μ C_{18}, 4.6 × 150 mm), the isolate also appeared as a single peak at 5.3 minutes, suggesting a single isolated component.

There are three biologically plausible positions for glucuronidation of 5HTOL; the C5 (phenolic) hydroxyl of the indole, the aliphatic hydroxyl, and the amine group of the indole (Fig. 4). The 1H-spectrum of the isolate when dissolved in DMSO-*d*6 contains two resonances at δ 10.78 and 10.67 that together integrate to a single hydrogen. The COSY spectrum contains cross peaks indicating these resonances are coupled to resonances at δ 7.18 and 7.11 (Fig. 4). When the sample is diluted in

DMD Fast Forward. Published on February 22, 2012 as DOI: 10.1124/dmd.111.043117
This article has not been copyedited and formatted. The final version may differ from this version.

methanol-*d*4, the δ 10.78 and 10.67 resonances are absent from both the 1H and COSY spectrum (Supplemental Fig. 1). Based on these data the δ 10.78 and 10.67 are assigned as the NH of the indole and eliminates this site as a potential site for glucuronidation.

The HMBC spectrum of the isolated sample diluted in methanol-*d*4 contains cross peaks that indicate long range coupling from the anomeric proton (δ 4.89 ppm) to a carbon with a chemical shift of 152.7 ppm. The HMBC data also contains cross peaks from two aromatic proton resonances at 7.33 and 7.25 ppm to the carbon at 152.7 ppm (Supplemental Fig. 2). This strongly indicates the 5HTOL is glucuronidated at the C5 (phenolic) position of the indole. The HMBC spectrum (diluted in methanol-*d*4) contains no evidence for any coupling of the anomeric proton to any aliphatic carbon. These combined data suggest a single site of glucuronidation of 5HTOL in human liver microsomes at the phenolic oxygen (Fig. 4). These experiments confirmed that of the three likely glucuronidation sites, the analogous serotonin 5-hydroxyl moiety was glucuronidated (Krishnaswamy et al., 2003).

Nonspecific Binding. The fraction of unbound substrate in incubation ($f_{u,inc}$) is shown in Table 4 and was determined at substrate concentrations close to K_m or S_{50} for ES (170 μM), TFP (67 μM), AZT (373 μM), or a concentration range for 5HTOL (3, 30, 300 μM) and PRO (4, 40 μM). Substrate recovery for all compounds met acceptance criteria and ranged 73-134%. ES is moderately bound (14% free) to HLMs at 0.025 mg/ml and highly bound (3.9% free) with the addition of 2% BSA. These values reflect significant microsomal binding even at low protein concentration and are in agreement with reported ES binding to BSA (9-11% free with 0.5% BSA) (Rowland et al., 2009) and high plasma protein binding (~2% free). TFP was moderately bound to HLM (28% free) and highly bound with 2% BSA (6.1% free) in agreement with previously reported microsomal binding at the concentration tested (Uchaipichat et al., 2006a). Previous studies indicated a degree of saturable protein binding for TFP in HLM between a concentration range of 10-200 μM, with $f_{u,inc}$ increasing from 0.21-0.59 (Uchaipichat et al., 2006a). Unbound TFP enzyme kinetic parameters reported in this study (Table 4) did not account for the possibility of saturable binding. 5HTOL was poorly bound to HLM (93% free) and HLM with BSA

DMD Fast Forward. Published on February 22, 2012 as DOI: 10.1124/dmd.111.043117
This article has not been copyedited and formatted. The final version may differ from this version.

(90% free) and mean $f_{u,inc}$ is reported in Table 4. The $f_{u,inc}$ in HLM at 3 μM, 30 μM, or 300 μM were 0.85, 0.98, and 0.95, respectively and for HLM with BSA 0.79, 0.94, and 0.97, respectively. PRO at 4 and 40 μM was not bound to HLM (100% free) and moderately bound with BSA (17% free) in agreement with previous HLM (70% free at 0.5 mg/ml) and BSA-binding studies (~20-60% free) (Rowland et al., 2008; Rowland et al., 2009). AZT exhibited moderate binding to HLM and HLM with BSA (69% free) in agreement with microsomal (60% free) and BSA binding (49% free) reported by Kilford et al., (2009), and reported AZT plasma protein binding of 62-66% free (product label) or 72-82% free (Luzier and Morse, 1993). A lower degree of AZT microsomal or BSA binding (≥ 90% free) was reported by other authors (Court et al., 2003; Rowland et al., 2007; Rowland et al., 2009).

β-Estradiol-3-Glucuronide Glucuronidation (UGT1A1). A LC-MS/MS assay for β-estradiol-3-glucuronosyltransferase, a probe substrate for UGT1A1 activity (Williams et al., 2002), was adopted and optimized for use at low protein concentrations. The resulting ES3-G product formation displayed atypical kinetics (curved Eadie-Hofstee plot) and best fit the Hill equation consistent with previous literature (Fisher et al., 2000). The mean Hill coefficient value (*n*), which gives an indication of the degree of sigmoidicity of the curve, ranged 1.8-2.7 for all incubation conditions (Table 3; Fig. 5), indicative of homotropic activation or positive cooperativity. The mean HLM and rUGT S_{50} values of 11 and 13 μM, respectively, is in agreement with apparent S_{50} values previously reported for HLMs ranging from 17-61 μM (Fisher et al., 2000; Alkharfy and Frye, 2002; Williams et al., 2002; Soars et al., 2003; Itäaho et al., 2008), and 8.7-23 μM for rUGT1A1 (Soars et al., 2003; Lepine et al., 2004; Fujiwara et al., 2007; Zhou et al., 2011).

In the presence of 2% BSA, total S_{50} increased (9- to 15-fold) with minor increases (1.3- to 1.7-fold) in V_{max}, resulting in decreased apparent CL_{max} (Table 3). However, when corrected for unbound kinetics (Table 4), S_{50} values were significantly lower (~8- to 26-fold) than total S_{50} and more comparable between HLM and rUGT (1.4-6.6 μM) due to a high degree of microsomal and BSA binding (Table 4).

DMD Fast Forward. Published on February 22, 2012 as DOI: 10.1124/dmd.111.043117
This article has not been copyedited and formatted. The final version may differ from this version.

The resultant HLM unbound maximal clearance ($CL_{max,u}$) decreased slightly with BSA addition, but was relatively similar (within 2.6-fold) to values obtained in the absence of BSA.

Trifluoperazine *N*-Glucuronidation (UGT1A4). A trifluoperazine-*N*-glucuronosyltransferase LC-MS/MS assay, which has been shown to be selective for measurement of UGT1A4 activity (Uchaipichat et al., 2006a) as previously quantified by LC/UV based on aglycone absorbance (Uchaipichat et al., 2006b), was developed. The structural identity of TFP-G isolated from *in vitro* HLM incubations were in agreement with the TFP-G analytical standard as compared by NMR spectroscopy (*data not shown*). The TFP-G product formation data in HLM and rUGT exhibited substrate inhibition kinetics (Table 3; Fig. 5) while HLM in the presence of BSA displayed Michaelis-Menten kinetics. Substrate concentrations higher than 200 μM failed to remain in solution in the absence of BSA, accordingly the 300 and 550 μM TFP concentrations were not used for determining apparent enzyme kinetic parameters; however solubility did not appear to be affected in the presence of BSA. The mean total and unbound K_m values in HLM were 42 μM and 11 μM, respectively, in agreement with K_m values reported in HLMs that have ranged from 35-84 μM or 4.7-7.6 μM when corrected for nonspecific binding (Uchaipichat et al., 2006a). In rUGT1A4 total and unbound K_m values were 15 and 4.1 μM, respectively, in agreement with reported rUGT1A4 values (binding corrected) of 20-44 (4.1) μM (Uchaipichat et al., 2006a; Fujiwara et al., 2007; Kubota et al., 2007; Kerdpin et al., 2009). When corrected for nonspecific binding, HLM unbound CL_{int} increased slightly (1.6-fold) due to a relatively higher degree of BSA binding (Table 4). Although unbound HLM K_m was comparable to previous reports, V_{max} was higher with a pronounced effect of BSA on rUGT1A4 V_{max}, comparable to observations with lamotrigine as UGT1A4 substrate (Rowland et al., 2006).

5-Hydroxytryptophol-*O*-Glucuronidation (UGT1A6). A 5-hydroxytryptophol-*O*-glucuronosyltransferase LC-MS/MS assay for UGT1A6 was developed and optimized. The 5HTOL-G formation displayed weak substrate inhibition kinetics (Table 3; Fig. 5). The mean K_m values in HLM and rUGT were 420 μM and 570 μM, respectively. Values cited for K_m in HLMs have ranged from 134-

DMD Fast Forward. Published on February 22, 2012 as DOI: 10.1124/dmd.111.043117
This article has not been copyedited and formatted. The final version may differ from this version.

156 μM, and 135 μM for rUGT1A6 (Krishnaswamy et al., 2004). In the presence of 2% BSA, unbound kinetic parameters (Table 4) did not change significantly, due to a low degree of nonspecific binding.

Propofol-*O*-Glucuronidation (UGT1A9). A propofol-*O*-glucuronosyltransferase LC/MS-MS assay was developed to evaluate UGT1A9 activities in HLMs and rUGT. The PRO-G product formation data displayed substrate inhibition kinetics except for data collected using HLMs in the presence of 2% BSA, which displayed Michaelis-Menten kinetics (Table 3; Fig. 6). The optimized method yielded mean K_m values of 98 μM and 200 μM for HLMs and rUGT1A9, respectively. Previously reported K_m values obtained in HLMs ranged 64-280 μM (Soars et al., 2003; Shimizu et al., 2007; Rowland et al., 2008) and 28-111 μM for rUGT1A9 (Soars et al., 2003; Rowland et al., 2008; Takahashi et al., 2008; Fujiwara et al., 2010). In the presence of 2% BSA, total K_m values for HLMs and rUGT1A9 were 46 μM and 63 μM for HLMs and rUGT1A9, respectively. Previously reported K_m values in the presence of BSA were 15.5 μM and 7.2 μM for HLM and rUGT, respectively (Rowland et al., 2008). As shown in Table 4, the addition of BSA resulted in significant increases in unbound CL_{int} (7.1-fold).

AZT-5′-Glucuronidation (UGT2B7). An AZT-5′-glucuronosyltransferase assay with LC-MS/MS detection (Engtrakul et al., 2005) was optimized to evaluate UGT2B7 activities in HLMs and rUGT as an established UGT2B7 probe substrate (Court et al., 2003). The AZT-G product formation data displayed Michaelis-Menten kinetics (Table 3; Fig. 6). Statistical evaluation (F-test) indicated a statistically better enzyme kinetic fit ($p < 0.05$) with a substrate inhibition model for incubation conditions, except for rUGT in the presence of BSA. However, visual inspection of the fit did not justify utilization of a more complex model and conclusive evidence would require incubation with substrate concentrations >4500 μM. The mean K_m values for HLM (840 μM), HLM with BSA (160 μM), and rUGT (1100 μM) estimated with the substrate inhibition model were comparable to those reported in Table 3, where the mean total K_m values for HLMs and rUGT2B7 were 610 μM and 900 μM, respectively. Values are in agreement with published K_m values in HLMs ranging from 518-1600 μM and for rUGT2B7 values of 478-770 μM have been reported (Court et al., 2003; Engtrakul et al., 2005; Uchaipichat et al., 2006b;

Peterkin et al., 2007; Rowland et al., 2009). In the presence of 2% BSA, mean K_m values for HLMs and rUGT2B7 were 150 μM and 320 μM, respectively. Previously reported K_m values in the presence of BSA were 69-105 μM and 40-70 μM for HLM and rUGT, respectively (Uchaipichat et al., 2006b; Rowland et al., 2007; Rowland et al., 2009). Corrections for unbound concentrations in microsomes resulted in slight decreases in K_m while addition of BSA decreased K_m (Table 4). Unbound HLM K_m (100 μM) with BSA was comparable to globulin-free BSA (188 μM) and reported values in the presence of crude BSA (87 μM) (Rowland et al., 2007). The decreases in unbound K_m (4.2-fold) and increases in V_{max} (2.2-fold) in the presence of BSA resulted in a significantly increased unbound HLM CL_{int} (9.2-fold) (Table 4).

UGT Inhibition. Eleven previously reported UGT inhibitors and known CYP inhibitors were screened at two concentrations (50 and 500 μM) for their ability to inhibit the five hepatic UGTs studied in order to evaluate a high-throughput UGT inhibitors screening scenario (Table 5). Activities were compared to solvent control. Chrysin significantly inhibited UGTs 1A1, 1A6, 1A9 and 2B7; diflunisal appeared to be selective as UGT1A9 inhibitor; mefenamic acid mostly inhibited UGTs 1A9 and 2B7; silybinin was most potent as UGT1A1 inhibitor; tangeretin inhibited UGT1A1 and 1A9. Valproic acid exhibited minimal UGT inhibition at 500 μM. The CYP inhibitor 1-aminobenzotriazole did not inhibit UGTs up to 500 μM while the other CYP inhibitors tested appeared to be nonselective inhibitors of UGTs 1A1 and 1A4 (itraconazole), UGTs 1A1, 1A4, and 2B7 (ketoconazole and ritonavir), and weak UGT1A1 inhibition by verapamil at 50 μM with nonselective inhibition at the higher concentration tested.

IC_{50} experiments (Table 6) with chrysin confirmed potent inhibition of UGT1A1 with less than 10-fold selectivity over UGTs 1A6, 1A9 and 2B7. Itraconazole is a potent inhibitor (IC_{50} < 1 μM) of UGTs 1A1 and 1A4, while activities of UGTs 1A6, 1A9 and 2B7 were unaffected up to 100 μM. The addition of BSA typically increased IC_{50} values, likely due to an increase in nonspecific inhibitor binding (not specifically measured in these studies), reflecting the importance of correcting IC_{50} or K_i values for nonspecific binding when attempting DDI predictions.

DMD Fast Forward. Published on February 22, 2012 as DOI: 10.1124/dmd.111.043117
This article has not been copyedited and formatted. The final version may differ from this version.

Discussion

Over the past couple of decades, major advances were made in the characterization of UGT enzyme substrate and inhibitor selectivities, highlighting the importance of glucuronidation in drug metabolism, *in vitro-in vivo* extrapolation of drug clearance, and prediction of DDIs (Miners et al., 2010a). The UGT reaction phenotyping techniques have progressed significantly with the identification and characterization of selective probe substrates, availability of recombinant UGTs, and optimization of *in vitro* incubation conditions required to measure drug glucuronidation. However, a serious shortcoming in the UGT reaction phenotyping process is the lack of isoform-selective inhibitors that could be used in liver microsomal incubations, analogous to those available for cytochrome P450 enzymes (Zhang et al., 2007). Selective UGT inhibitor probes are limited to hecogenin (UGT1A4), niflumic acid (UGT1A9), and fluconazole (UGT2B7) (Miners et al., 2010a). Thus, the confidence in UGT reaction phenotyping could benefit significantly from the identification of a greater number of enzyme-selective inhibitors for UGTs that contribute to hepatic drug metabolism. Accordingly, highly selective, robust, and sensitive LC-MS/MS analytical techniques would assist high-throughput screening efforts to increase future success in this endeavor.

Glucuronidation reactions have been described to be impacted significantly by *in vitro* incubation conditions such as buffer type and ionic strength, latency, glucuronide stability, atypical kinetics, and the albumin effect (refer to *Introduction*). Some standardization occurred over time but universally accepted incubation conditions are not generally available with phosphate and Tris buffers used interchangeably for *in vitro* UGT reactions, while some authors noted highest AZT glucuronidation activity with a physiologically relevant carbonate buffer or Williams E medium (Engtrakul et al., 2005). In this study, Tris buffer provided greater activity for UGTs 1A4 and 1A9 in HLMs while all rUGT activities, except rUGT1A6, were increased relative to phosphate buffer. Similar findings were observed for acetaminophen glucuronidation with rUGT1A9 (Mutlib et al., 2006) and negligible impact of Tris on UGT1A1 (ES) (Soars et al., 2003) or UGT2B7 (AZT) (Boase and Miners, 2002; Engtrakul et al., 2005) activities. Boase and Miners (2002) demonstrated a trend of higher apparent V_{max} for AZT

DMD Fast Forward. Published on February 22, 2012 as DOI: 10.1124/dmd.111.043117
This article has not been copyedited and formatted. The final version may differ from this version.

glucuronidation in Tris compared to phosphate buffers and interestingly, a significant decrease in CL_{int} at higher phosphate ionic strength (20-100 mM), primarily due to an increase in apparent K_m. The mechanistic effect or impact of phosphate on UGT activity is not completely clear, although altered substrate selectivity and activity have been reported due to UGT phosphorylation (Basu et al., 2005).

Divalent metal ions increase UGT activity and $MgCl_2$ (2-10 mM) is typically included in *in vitro* UGT incubations, with some utilizing $MgCl_2$ concentrations closer the endoplasmic reticulum interior (1 mM) or as high as 50 mM (Fisher et al., 2001). Inclusion of $MgCl_2$ increased UGT activities by ~2- to 8-fold in HLMs and to a lesser extent in rUGTs with 5 mM generally resulting in maximal stimulation of glucuronidation. A final $MgCl_2$ concentration of 5 mM for the optimized incubation conditions is in agreement with general practice (4-5 mM) (Boase and Miners, 2002; Court, 2004). Saccharolactone, an inhibitor of endogenous β-glucuronidase-catalysed hydrolysis of the glucuronide conjugate is often added to UGT incubations and in some cases is required to preserve glucuronide stability (Bauman et al., 2005). In this study, saccharolactone did not increase glucuronide formation and it occasionally decreased glucuronidation (e.g. UGTs 1A4, 1A9). These findings are in agreement with reports indicating limited saccharolactone benefit or an inhibitory effect (Kaivosaari et al., 2008; Oleson and Court, 2008).

Alamethicin, a pore-forming peptide, is currently the preferred agent to activate microsomal UGT activity, presumably by increasing access of substrate and cofactor to the luminal orientation of UGT proteins (Fisher et al., 2001). A standard alamethicin concentration of 50 µg/mg microsomal protein is routinely used based on optimization (50-100 µg alamethicin/mg HLM) with microsomal protein concentrations ranging 0.5-2.5 mg/ml (Fisher et al., 2000) and other supportive studies (Kaivosaari et al., 2008). Activation in hepatocytes required higher alamethicin concentrations (≥200 µg/ml) (Banhegyi et al., 1993). Development of LC-MS/MS analytical methods allows utilization of lower protein concentrations in incubation and initial optimization (0.01-0.1 mg/ml HLM) indicated a lack of linearity in glucuronide product formation using standard alamethicin activation conditions (50 µg/mg). Further evaluation of optimal alamethicin concentration (2-2500 µg/mg HLMs) indicated dependence of the critical alamethicin activation concentration on microsomal protein concentration and loss of activation at

low protein concentrations (Table 2 and Fig. 3), even with alamethicin levels as high as 292 µg/mg microsomal protein. Accordingly, maximal activation could occur with as little as 17.1 µg/mg HLMs at high HLM protein concentration while lower HLM protein incubations may require as much as 855 µg alamethicin/mg protein. Hence, in order to standardize, it is more appropriate to express optimal alamethicin activation concentrations as µg/ml in the incubation, especially when employing HLM protein concentrations <0.2 mg/ml (Fig. 3). The exact reason for this phenomenon is not clear, but it is apparent that a critical alamethicin concentration in solution is required for optimal activation, independent of protein concentration. The current recommendation is to use a standard alamethicin activation concentration of at least 10 µg/ml incubate for microsomal protein concentrations between 0.01-0.5 mg/ml. Conversely, although alamethicin is often included in incubations of insect cell baculoviral-expressed UGTs, no activation was observed in this study suggesting little benefit consistent with similar reports (Kaivosaari et al., 2008).

Enzyme kinetic parameters, for UGTs 1A9 and 2B7 were most significantly impacted by the addition of 2% BSA while UGTs 1A1, 1A4 and 1A6 were affected to a lesser degree. In general, total K_m or S_{50} increased for UGT 1A1 and 1A4, remained unchanged for UGT1A6, and decreased for UGT 1A9 and 2B7 while apparent V_{max} remained relatively unaffected (< 2-fold change). When corrected for nonspecific binding in the incubation, the unbound $CL_{int,}$ in the presence of BSA increased most significantly for UGTs 1A9 and 2B7, and remained relatively unaffected for other UGTs investigated. Previous studies indicated that BSA decreased PRO K_m without impacting V_{max} in HLM and rUGT with similar observations for AZT in HLM (Rowland et al., 2008; Rowland et al., 2009). A more recent study indicated decreases in K_m but significant increases in V_{max} for entacapone (UGT1A9) and only decreases in the K_m for AZT in HLM and rUGT (Manevski et al., 2011). These findings indicate more complex mechanisms other that competitive inhibition by fatty acids may be involved in the inhibition of enzyme activity released from membranes. It has been postulated that the albumin effect is impacted by enzyme source or differing fatty acid composition released from membranes (Rowland et al., 2008; Rowland et al., 2009), which could result in differences in apparent kinetic parameter estimates for HLM or rUGT,

DMD Fast Forward. Published on February 22, 2012 as DOI: 10.1124/dmd.111.043117
This article has not been copyedited and formatted. The final version may differ from this version.

but comparisons between human embryonic kidney (HEK293) and *Spodoptera frugiperda* (S*f*9) expression systems does not explain the observations for entacapone (Manevski et al., 2011). It should also be noted that *in vitro* CL_{int} could differ depending on microsomal enzyme source due to significant inter-individual variation of AZT glucuronidation rates (Peterkin et al., 2007), and apparent V_{max} estimates determined without an authentic glucuronide standard (Rowland et al., 2007).

The S_{50} for UGT1A1 catalyzed ES glucuronidation reported in this study (1.4-6.6 μM) is significantly lower than previous observations for apparent ES S_{50} (17-61 μM) (Fisher et al., 2000; Itäaho et al., 2008) due to considerable microsomal binding even when employing a low protein concentration in incubation, reiterating the importance of correcting for nonspecific binding in kinetic parameter estimates. Although glucuronidation is often considered to be a low affinity process (Williams et al., 2004), high micromolar affinity for ES and TFP (4.1-11 μM) was observed similar to other reports for UGT1A substrates (Goosen et al., 2007; Liu et al., 2010).

Inhibition of UGT activities was confirmed with potential UGT and characterized CYP inhibitors, which indicated non-selective inhibition by chrysin, mefenamic acid, silybinin, and tangeretin. Diflunisal may be a potent and selective UGT1A9 inhibitor but requires further characterization since weak UGT2B7 inhibition (IC_{50} 370 μM) was previously reported (Knights et al., 2009). Non-selective UGT inhibition was apparent with ketoconazole, itraconazole, ritonavir, and verapamil in agreement with previous reports on ketoconazole (Liu et al., 2011; Zhou et al., 2011). Of the CYP inhibitors investigated, minimal inhibition was observed with the pan-CYP inhibitor 1-aminobenzotriazole, which indicated it may be useful when phenotyping mixed UGT and CYP substrates and estimating fractional metabolism (f_m) by CYP vs UGT (Kilford et al., 2009).

In summary, we describe optimized *in vitro* incubation and alamethicin activation conditions, LC-MS/MS analytical methods utilizing authentic glucuronide standards, and kinetic parameters for five hepatic UGTs. These methods should prove useful in the routine assessments of the potential for new drug candidates to elicit pharmacokinetic drug interactions via inhibition of human UGT activities and

advantageous when screening larger compound libraries to identify UGT-enzyme selective chemical inhibitors.

Acknowledgements

The authors would like to acknowledge Dr. Brian Ethell for helpful scientific discussions, and Howard Miller and Mark Snyder for experimental assistance with the high-throughput experimental automation.

Authorship Contributions

Participated in research design: Walsky, Bauman, Lapham, Bourcier, Giddens, Obach, Hyland, and Goosen.

Conducted experiments: Walsky, Bauman, Lapham, Bourcier, Giddens, Negahban, Hyland, and Ryder.

Contributed new reagents or analytical tools: Walsky, Bauman, Lapham, Bourcier, Giddens, Negahban, Ryder.

Performed data analysis: Walsky, Bauman, Lapham, Bourcier, Giddens, Negahban, Ryder, Hyland, and Goosen.

Wrote or contributed to the writing of the manuscript: Walsky, Bauman, Lapham, Bourcier, Giddens, Negahban, Ryder, Obach, Hyland, and Goosen.

References

Alkharfy KM and Frye RF (2002) Sensitive liquid chromatographic method using fluorescence detection for the determination of estradiol 3- and 17-glucuronides in rat and human liver microsomal incubations: formation kinetics. *J Chromatogr B Analyt Technol Biomed Life Sci* **774:**33-38.

Banhegyi G, Garzo T, Fulceri R, Benedetti A, and Mandl J (1993) Latency is the major determinant of UDP-glucuronosyltransferase activity in isolated hepatocytes. *FEBS Lett* **328:**149-152.

Basu NK, Kovarova M, Garza A, Kubota S, Saha T, Mitra PS, Banerjee R, Rivera J, and Owens IS (2005) Phosphorylation of a UDP-glucuronosyltransferase regulates substrate specificity. *Proc Natl Acad Sci U S A* **102:**6285-6290.

Bauman JN, Goosen TC, Tugnait M, Peterkin V, Hurst SI, Menning LC, Milad M, Court MH, and Williams JA (2005) UDP-glucuronosyltransferase 2B7 is the major enzyme responsible for gemcabene glucuronidation in human liver microsomes. *Drug Metab Dispos* **33:**1349-1354.

Bjornsson TD, Callaghan JT, Einolf HJ, Fischer V, Gan L, Grimm S, Kao J, King SP, Miwa G, Ni L, Kumar G, McLeod J, Obach RS, Roberts S, Roe A, Shah A, Snikeris F, Sullivan JT, Tweedie D, Vega JM, Walsh J, and Wrighton SA (2003) The conduct of in vitro and in vivo drug-drug interaction studies: a Pharmaceutical Research and Manufacturers of America (PhRMA) perspective. *Drug Metab Dispos* **31:**815-832.

Boase S and Miners JO (2002) In vitro-in vivo correlations for drugs eliminated by glucuronidation: investigations with the model substrate zidovudine. *Br J Clin Pharmacol* **54:**493-503.

Court MH (2004) In vitro identification of UDP-glucuronosyl-transferases (UGTs) involved in drug metabolism, in: *Optimization in Drug Discovery* (Yan Z and Caldwell GW eds), pp 185-202, Humana Press Inc., Totowa, N. J.

Court MH (2005) Isoform-selective probe substrates for in vitro studies of human UDP-glucuronosyltransferases. *Methods Enzymol* **400:**104-116.

Court MH (2010) Interindividual variability in hepatic drug glucuronidation: studies into the role of age, sex, enzyme inducers, and genetic polymorphism using the human liver bank as a model system. *Drug Metab Rev* **42:**209-224.

Court MH, Krishnaswamy S, Hao Q, Duan SX, Patten CJ, Von Moltke LL, and Greenblatt DJ (2003) Evaluation of 3'-azido-3'-deoxythymidine, morphine, and codeine as probe substrates for UDP-glucuronosyltransferase 2B7 (UGT2B7) in human liver microsomes: specificity and influence of the UGT2B7*2 polymorphism. *Drug Metab Dispos* **31:**1125-1133.

Donato MT, Montero S, Castell JV, Gomez-Lechon MJ, and Lahoz A (2010) Validated assay for studying activity profiles of human liver UGTs after drug exposure: inhibition and induction studies. *Anal Bioanal Chem* **396:**2251-2263.

Easterbrook J, Lu C, Sakai Y, and Li AP (2001) Effects of organic solvents on the activities of cytochrome P450 isoforms, UDP-dependent glucuronyl transferase, and phenol sulfotransferase in human hepatocytes. *Drug Metab Dispos* **29:**141-144.

Engtrakul JJ, Foti RS, Strelevitz TJ, and Fisher MB (2005) Altered AZT (3'-azido-3'-deoxythymidine) glucuronidation kinetics in liver microsomes as an explanation for underprediction of in vivo clearance: comparison to hepatocytes and effect of incubation environment. *Drug Metab Dispos* **33:**1621-1627.

Fisher MB, Campanale K, Ackermann BL, VandenBranden M, and Wrighton SA (2000) In vitro glucuronidation using human liver microsomes and the pore-forming peptide alamethicin. *Drug Metab Dispos* **28:**560-566.

Fisher MB, Paine MF, Strelevitz TJ, and Wrighton SA (2001) The role of hepatic and extrahepatic UDP-glucuronosyltransferases in human drug metabolism. *Drug Metab Rev* **33:**273-297.

Fujiwara R, Nakajima M, Oda S, Yamanaka H, Ikushiro S, Sakaki T, and Yokoi T (2010) Interactions between human UDP-glucuronosyltransferase (UGT) 2B7 and UGT1A enzymes. *J Pharm Sci* **99:**442-454.

Fujiwara R, Nakajima M, Yamanaka H, Katoh M, and Yokoi T (2007) Interactions between human UGT1A1, UGT1A4, and UGT1A6 affect their enzymatic activities. *Drug Metab Dispos* **35:**1781-1787.

Goosen TC, Bauman JN, Davis JA, Yu C, Hurst SI, Williams JA, and Loi CM (2007) Atorvastatin glucuronidation is minimally and nonselectively inhibited by the fibrates gemfibrozil, fenofibrate, and fenofibric acid. *Drug Metab Dispos* **35:**1315-1324.

Houston JB and Kenworthy KE (2000) In vitro-in vivo scaling of CYP kinetic data not consistent with the classical Michaelis-Menten model. *Drug Metab Dispos* **28:**246-254.

Itäaho K, Mackenzie PI, Ikushiro S, Miners JO, and Finel M (2008) The configuration of the 17-hydroxy group variably influences the glucuronidation of beta-estradiol and epiestradiol by human UDP-glucuronosyltransferases. *Drug Metab Dispos* **36:**2307-2315.

Kaivosaari S, Toivonen P, Aitio O, Sipila J, Koskinen M, Salonen JS, and Finel M (2008) Regio- and stereospecific N-glucuronidation of medetomidine: the differences between UDP glucuronosyltransferase (UGT) 1A4 and UGT2B10 account for the complex kinetics of human liver microsomes. *Drug Metab Dispos* **36:**1529-1537.

Kerdpin O, Mackenzie PI, Bowalgaha K, Finel M, and Miners JO (2009) Influence of N-terminal domain histidine and proline residues on the substrate selectivities of human UDP-glucuronosyltransferase 1A1, 1A6, 1A9, 2B7, and 2B10. *Drug Metab Dispos* **37:**1948-1955.

Kiang TK, Ensom MH, and Chang TK (2005) UDP-glucuronosyltransferases and clinical drug-drug interactions. *Pharmacol Ther* **106:**97-132.

Kilford PJ, Stringer R, Sohal B, Houston JB, and Galetin A (2009) Prediction of drug clearance by glucuronidation from in vitro data: use of combined cytochrome P450 and UDP-glucuronosyltransferase cofactors in alamethicin-activated human liver microsomes. *Drug Metab Dispos* **37:**82-89.

Knights KM, Winner LK, Elliot DJ, Bowalgaha K, and Miners JO (2009) Aldosterone glucuronidation by human liver and kidney microsomes and recombinant UDP-glucuronosyltransferases: inhibition by NSAIDs. *Br J Clin Pharmacol* **68:**402-412.

Krishnaswamy S, Duan SX, Von Moltke LL, Greenblatt DJ, Sudmeier JL, Bachovchin WW, and Court MH (2003) Serotonin (5-hydroxytryptamine) glucuronidation in vitro: assay development, human liver microsome activities and species differences. *Xenobiotica* **33:**169-180.

Krishnaswamy S, Hao Q, Von Moltke LL, Greenblatt DJ, and Court MH (2004) Evaluation of 5-hydroxytryptophol and other endogenous serotonin (5-hydroxytryptamine) analogs as substrates for UDP-glucuronosyltransferase 1A6. *Drug Metab Dispos* **32:**862-869.

Kubota T, Lewis BC, Elliot DJ, Mackenzie PI, and Miners JO (2007) Critical roles of residues 36 and 40 in the phenol and tertiary amine aglycone substrate selectivities of UDP-glucuronosyltransferases 1A3 and 1A4. *Mol Pharmacol* **72:**1054-1062.

Lepine J, Bernard O, Plante M, Tetu B, Pelletier G, Labrie F, Belanger A, and Guillemette C (2004) Specificity and regioselectivity of the conjugation of estradiol, estrone, and their catecholestrogen and methoxyestrogen metabolites by human uridine diphospho-glucuronosyltransferases expressed in endometrium. *J Clin Endocrinol Metab* **89:**5222-5232.

Liu Y, Ramirez J, House L, and Ratain MJ (2010) Comparison of the drug-drug interactions potential of erlotinib and gefitinib via inhibition of UDP-glucuronosyltransferases. *Drug Metab Dispos* **38:**32-39.

Liu Y, She M, Wu Z, and Dai R (2011) The inhibition study of human UDP-glucuronosyltransferases with cytochrome P450 selective substrates and inhibitors. *J Enzyme Inhib Med Chem* **26:**386-393.

Luzier A and Morse GD (1993) Intravascular distribution of zidovudine: role of plasma proteins and whole blood components. *Antiviral Res* **21:**267-280.

Mackenzie PI, Bock KW, Burchell B, Guillemette C, Ikushiro S, Iyanagi T, Miners JO, Owens IS, and Nebert DW (2005) Nomenclature update for the mammalian UDP glycosyltransferase (UGT) gene superfamily. *Pharmacogenet Genomics* **15:**677-685.

Manevski N, Moreolo PS, Yli-Kauhaluoma J, and Finel M (2011) Bovine serum albumin decreases Km values of human UDP-glucuronosyltransferases 1A9 and 2B7 and increases Vmax values of UGT1A9. *Drug Metab Dispos* **39:**2117-2129.

Miners JO, Mackenzie PI, and Knights KM (2010a) The prediction of drug-glucuronidation parameters in humans: UDP-glucuronosyltransferase enzyme-selective substrate and inhibitor probes for reaction phenotyping and in vitro-in vivo extrapolation of drug clearance and drug-drug interaction potential. *Drug Metab Rev* **42:**196-208.

Miners JO, Polasek TM, Mackenzie PI, and Knights KM (2010b) The in vitro characterization of inhibitory drug-drug interactions involving UDP - glucuronosyltransferase, in: *Enzyme- and Transporter-Based Drug-Drug Interactions: Progress and Future Challenges* (Pang KS, Rodrigues AD, and Peter RM eds), pp 217-236, Springer, New York, N. Y.

Mutlib AE, Goosen TC, Bauman JN, Williams JA, Kulkarni S, and Kostrubsky S (2006) Kinetics of acetaminophen glucuronidation by UDP-glucuronosyltransferases 1A1, 1A6, 1A9 and 2B15. Potential implications in acetaminophen-induced hepatotoxicity. *Chem Res Toxicol* **19:**701-709.

Oleson L and Court MH (2008) Effect of the beta-glucuronidase inhibitor saccharolactone on glucuronidation by human tissue microsomes and recombinant UDP-glucuronosyltransferases. *J Pharm Pharmacol* **60:**1175-1182.

Parkinson A, Kazmi F, Buckley DB, Yerino P, Ogilvie BW, and Paris BL (2010) System-dependent outcomes during the evaluation of drug candidates as inhibitors of cytochrome P450 (CYP) and uridine diphosphate glucuronosyltransferase (UGT) enzymes: human hepatocytes versus liver microsomes versus recombinant enzymes. *Drug Metab Pharmacokinet* **25:**16-27.

Peterkin VC, Bauman JN, Goosen TC, Menning L, Man MZ, Paulauskis JD, Williams JA, and Myrand SP (2007) Limited influence of UGT1A1*28 and no effect of UGT2B7*2 polymorphisms on UGT1A1 or UGT2B7 activities and protein expression in human liver microsomes. *Br J Clin Pharmacol* **64:**458-468.

Rowland A, Elliot DJ, Williams JA, Mackenzie PI, Dickinson RG, and Miners JO (2006) In vitro characterization of lamotrigine N2-glucuronidation and the lamotrigine-valproic acid interaction. *Drug Metab Dispos* **34:**1055-1062.

Rowland A, Gaganis P, Elliot DJ, Mackenzie PI, Knights KM, and Miners JO (2007) Binding of inhibitory fatty acids is responsible for the enhancement of UDP-glucuronosyltransferase 2B7 activity by albumin: implications for in vitro-in vivo extrapolation. *J Pharmacol Exp Ther* **321:**137-147.

Rowland A, Knights KM, Mackenzie PI, and Miners JO (2008) The "albumin effect" and drug glucuronidation: bovine serum albumin and fatty acid-free human serum albumin enhance the glucuronidation of UDP-glucuronosyltransferase (UGT) 1A9 substrates but not UGT1A1 and UGT1A6 activities. *Drug Metab Dispos* **36:**1056-1062.

Rowland A, Knights KM, Mackenzie PI, and Miners JO (2009) Characterization of the binding of drugs to human intestinal fatty acid binding protein (IFABP): potential role of IFABP as an alternative to albumin for in vitro-in vivo extrapolation of drug kinetic parameters. *Drug Metab Dispos* **37:**1395-1403.

Shimizu M, Matsumoto Y, and Yamazaki H (2007) Effects of propofol analogs on glucuronidation of propofol, an anesthetic drug, by human liver microsomes. *Drug Metab Lett* **1:**77-79.

Soars MG, Petullo DM, Eckstein JA, Kasper SC, and Wrighton SA (2004) An assessment of UDP-glucuronosyltransferase induction using primary human hepatocytes. *Drug Metab Dispos* **32:**140-148.

Soars MG, Ring BJ, and Wrighton SA (2003) The effect of incubation conditions on the enzyme kinetics of UDP-glucuronosyltransferases. *Drug Metab Dispos* **31:**762-767.

Takahashi H, Maruo Y, Mori A, Iwai M, Sato H, and Takeuchi Y (2008) Effect of D256N and Y483D on propofol glucuronidation by human uridine 5'-diphosphate glucuronosyltransferase (UGT1A9). *Basic Clin Pharmacol Toxicol* **103:**131-136.

Toffoli G, Cecchin E, Corona G, Russo A, Buonadonna A, D'Andrea M, Pasetto LM, Pessa S, Errante D, De Pangher V, Giusto M, Medici M, Gaion F, Sandri P, Galligioni E, Bonura S, Boccalon M, Biason P, and Frustaci S (2006) The role of UGT1A1*28 polymorphism in the pharmacodynamics and pharmacokinetics of irinotecan in patients with metastatic colorectal cancer. *J Clin Oncol* **24:**3061-3068.

Tsoutsikos P, Miners JO, Stapleton A, Thomas A, Sallustio BC, and Knights KM (2004) Evidence that unsaturated fatty acids are potent inhibitors of renal UDP-glucuronosyltransferases (UGT): kinetic studies using human kidney cortical microsomes and recombinant UGT1A9 and UGT2B7. *Biochem Pharmacol* **67:**191-199.

Uchaipichat V, Mackenzie PI, Elliot DJ, and Miners JO (2006a) Selectivity of substrate (trifluoperazine) and inhibitor (amitriptyline, androsterone, canrenoic acid, hecogenin, phenylbutazone, quinidine, quinine, and sulfinpyrazone) "probes" for human udp-glucuronosyltransferases. *Drug Metab Dispos* **34:**449-456.

Uchaipichat V, Mackenzie PI, Guo XH, Gardner-Stephen D, Galetin A, Houston JB, and Miners JO (2004) Human UDP-glucuronosyltransferases: isoform selectivity and kinetics of 4-methylumbelliferone and 1-naphthol glucuronidation, effects of organic solvents, and inhibition by diclofenac and probenecid. *Drug Metab Dispos* **32:**413-423.

Uchaipichat V, Winner LK, Mackenzie PI, Elliot DJ, Williams JA, and Miners JO (2006b) Quantitative prediction of in vivo inhibitory interactions involving glucuronidated drugs from in vitro data: the effect of fluconazole on zidovudine glucuronidation. *Br J Clin Pharmacol* **61:**427-439.

Venkatakrishnan K, von Moltke LL, Court MH, Harmatz JS, Crespi CL, and Greenblatt DJ (2000) Comparison between cytochrome P450 (CYP) content and relative activity approaches to scaling from cDNA-expressed CYPs to human liver microsomes: ratios of accessory proteins as sources of discrepancies between the approaches. *Drug Metab Dispos* **28:**1493-1504.

Walker GS, Ryder TF, Sharma R, Smith EB, and Freund A (2011) Validation of isolated metabolites from drug metabolism studies as analytical standards by quantitative NMR. *Drug Metab Dispos* **39:**433-440.

Walsky RL and Obach RS (2004) Validated assays for human cytochrome P450 activities. *Drug Metab Dispos* **32:**647-660.

Waters NJ, Jones R, Williams G, and Sohal B (2008) Validation of a rapid equilibrium dialysis approach for the measurement of plasma protein binding. *J Pharm Sci* **97:**4586-4595.

Williams JA, Andersson T, Andersson TB, Blanchard R, Behm MO, Cohen N, Edeki T, Franc M, Hillgren KM, Johnson KJ, Katz DA, Milton MN, Murray BP, Polli JW, Ricci D, Shipley LA, Vangala S, and Wrighton SA (2008) PhRMA white paper on ADME pharmacogenomics. *J Clin Pharmacol* **48:**849-889.

Williams JA, Hyland R, Jones BC, Smith DA, Hurst S, Goosen TC, Peterkin V, Koup JR, and Ball SE (2004) Drug-drug interactions for UDP-glucuronosyltransferase substrates: a pharmacokinetic explanation for typically observed low exposure (AUCi/AUC) ratios. *Drug Metab Dispos* **32:**1201-1208.

Williams JA, Ring BJ, Cantrell VE, Campanale K, Jones DR, Hall SD, and Wrighton SA (2002) Differential modulation of UDP-glucuronosyltransferase 1A1 (UGT1A1)-catalyzed estradiol-3-glucuronidation by the addition of UGT1A1 substrates and other compounds to human liver microsomes. *Drug Metab Dispos* **30:**1266-1273.

Zhang H, Davis CD, Sinz MW, and Rodrigues AD (2007) Cytochrome P450 reaction-phenotyping: an industrial perspective. *Expert Opin Drug Metab Toxicol* **3:**667-687.

Zhang L, Reynolds KS, Zhao P, and Huang SM (2010) Drug interactions evaluation: an integrated part of risk assessment of therapeutics. *Toxicol Appl Pharmacol* **243:**134-145.

Zhou J, Tracy TS, and Remmel RP (2011) Correlation between bilirubin glucuronidation and estradiol-3-gluronidation in the presence of model UDP-glucuronosyltransferase 1A1 substrates/inhibitors. *Drug Metab Dispos* **39:**322-329.

Footnotes

Presented in part at the 17th North American International Society for the Study of Xenobiotics (ISSX) meeting in Atlanta, Georgia, October 16-20, 2011.

Current address: Robert L. Walsky, Department of Drug Metabolism and Pharmacokinetics, AstraZeneca Pharmaceuticals LP, Waltham, Massachusetts.

Figure Legends

Figure 1. Major reactions catalyzed by human UDP-glucuronosyltransferase enzymes. Internal standards for LC-MS/MS analytical methods shown for each reaction.

Figure 2. Effect of incubation conditions on major human hepatic UGT activities in (A-C) pooled human liver microsomes, (D-F) and recombinantly expressed UGT enzymes. Values expressed as fold increase above activity (A, D) in presence of phosphate buffer, (B, E) absence of $MgCl_2$, or (C, F) absence of saccharolactone.

Figure 3. Optimal alamethicin concentration for activation of AZT glucuronidation in human liver microsomes. AZT-G formation shown at four concentrations (0.01 – 0.5 mg/ml) of pooled HLMs vs. alamethicin concentration expressed as (*panel A*) µg alamethicin per ml of incubate. The same data were also plotted expressing alamethicin concentration as (*panel B*) µg alamethicin per mg microsomal protein. Dashed lines signify (*panel A*) the current recommended optimal alamethicin activation concentration (10 µg/ml) and (*panel B*) the previously utilized alamethicin activation concentration (50 µg/mg). Corresponding data for β-estradiol and trifluoperazine glucuronidation are shown in Table 2.

Figure 4. Structure of 5-hydroxytryptophol-*O*-glucuronide showing NMR HMBC coupling at positions A, B, and C, which confirm glucuronidation at the phenolic 5-hydroxytryptophol position.

Figure 5. Enzyme kinetics of β-estradiol-3-glucuronide (UGT1A1), trifluoperazine-*N*-glucuronide (UGT1A4), and 5-hydroxytryptophol-*O*-glucuronide (UGT1A6) formation in pooled HLMs (*panel A, C, E*) or recombinant UGTs (*panel B, D, F*) in the absence and presence of 2% BSA. ES3-G formation displayed atypical kinetics as elucidated by the insert at low substrate concentrations in *panel B.* TFP-G and 5HTOL-G formation displayed substrate inhibition kinetics except TFP-G formation with HLMs in

presence of 2% BSA, which displayed Michaelis-Menten kinetics. Enzyme kinetic parameters and incubation conditions are summarized in Tables 2 and 3.

Figure 6. Enzyme kinetics of propofol-*O*-glucuronide and AZT-5′-glucuronide formation in pooled HLMs (*panel A, C*) or recombinant UGTs (*panel B, D*) in the absence and presence of 2% BSA. PRO-G formation displayed substrate inhibition kinetics except with HLMs in the presence of 2% BSA, which displayed Michaelis-Menten kinetics. AZT-G formation displayed Michaelis-Menten kinetics. Enzyme kinetic parameters and incubation conditions are summarized in Tables 2 and 3.

TABLE 1. Incubation conditions and analytical parameters for human UDP-glucuronosyltransferase assays

Assay	UGT1A1	UGT1A4	UGT1A6	UGT1A9	UGT2B7
Incubation Conditions:					
Human Liver Microsomes					
Protein Conc. (mg/ml)	0.025	0.025	0.025	0.025	0.025
Incubation Time (min)	60	30	20	30	60
Recombinant UGT					
Protein Conc. (mg/ml)	0.025	0.025	0.025	0.025	0.025
Incubation Time (min)	45	45	90	30	60
Analytical Conditions:					
Analyte	ES3-G	TFP-G	5HTOL-G	PRO-G	AZT-G
Internal Standard: Identity	1-naphthyl-*O*-glucuronide	[D_3]TFP-G	Diclofenac	Diclofenac	[$^{13}C_6$]AZT-G
Internal Standard Conc. (µM)	5.0	3.0	0.24	0.42	1.0
Injection Volume (µl)	20	20	10	20	10
Flow (ml/min)	0.4	0.75	1.0	0.6	0.5
Gradient Program, %B (min)	29(0) → 29(2) → 98(4.1)	10(0) → 2(0.1) → 80(2.0)	20(0) → 95(1.6) → 95(1.8)	90(0) → 90(1.2) → 97(4.4)	2(0) → 2(0.5) → 35(2.6)
Mass Spectrometer [a]	Sciex (1)	Sciex (1)	Sciex (2)	Sciex (2)	Waters (3)
Mass Spectrometer Conditions					
Detection Mode	negative	positive	negative	negative	negative
Ion Spray/Capillary Voltage	-4.50 kV	5.00 kV	-4.20 kV	-3.00 kV	-3.00 kV
Declustering/Cone Voltage	-55 eV	75 eV	30 eV	40 eV	-80 eV
Source/Desolvation Temperature	400°C	500°C	700°C	650°C	325°C
Collision Energy	-30 eV	45 eV	-35 eV	-30 eV	-26 eV
Analyte *m/z* Transition	447→113	584→408	352→176	353→177	442→125
Internal Standard *m/z* Transition	319→113	587→411	294→249	294→249	448→125
R_t: Analyte (min)	1.3	1.2	1.4	1.3	2.0
R_t: Internal Standard (min)	1.1	1.1	1.1	1.1	2.0
Standard Curve Range (nM)	20 – 2500	17 – 4300	5.0 – 2000	56 – 28000	50 – 5000
Accuracy (%)[b,c]	89.3	101	112	101	101
Precision (%)[b,d]	8.6	11	12	7.5	5.1

m/z, mass to charge; R_t, retention time.

[a] Analytical quantification were conducted by LC-MS/MS using three systems as described under *Materials and Methods*.

[b] Determined at 2nd lowest analytical standard concentration.

[c] Accuracy (%) = 100 • $[analyte]_{measured}/[analyte]_{nominal}$.

[d] Precision (%) = 100 • S.D. $[analyte]_{measured}/[analyte]_{measured}$.

TABLE 2. Optimal alamethicin concentration for activation of β-estradiol (UGT1A1) and trifluoperazine (UGT1A4) glucuronidation in human liver microsomes

	Alamethicin concentration [a]					β-Estradiol-3-glucuronide				Trifluoperazine *N*-glucuronide			
	μg/ml	*μg/mg HLM protein*				*μM*				*μM*			
HLM conc. (mg/ml)	0.01-0.5	0.01	0.05	0.2	0.5	0.01	0.05	0.2	0.5	0.01	0.05	0.2	0.5
	0	0	0	0	0	0.20	0.79	2.6	3.5	0.28	1.3	3.4	4.8
	1.0	100	20	5.0	2.0	0.17	0.77	2.2	3.3	0.29	1.4	3.5	4.8
	1.71	171	34.2	8.55	3.42	0.18	0.79	2.3	3.3	0.28	1.4	3.5	4.6
	2.92	292	58.4	14.6	5.84	0.19	0.88	2.2	3.4	0.31	1.5	3.5	4.7
	5.0	500	100	25	10	0.28	1.3	3.4	4.1	0.44	2.2	4.6	5.5
	8.55	855	171	42.8	17.1	0.32	1.5	3.4	4.6	0.52	2.6	5.2	6.4
	14.6	1460	292	73	29.2	0.32	1.4	3.7	4.7	0.51	2.6	5.2	6.6
	25	2500	500	125	50	0.27	1.2	3.3	4.5	0.47	2.5	5.3	6.8

[a] HLM was incubated without and with alamethicin at a constant concentration ranging 1-25 μg/ml at four HLM protein concentrations ranging 0.01-0.5 mg/ml as described under *Materials and Methods.* Based on the HLM concentration in incubation, the corresponding alamethicin concentration expressed as μg/mg HLM protein ranges 100-2500 μg/mg for 0.01 mg/ml HLM and 2-50 μg/mg for 0.5 mg/ml HLM.

TABLE 3. Kinetic parameters for human UDP-glucuronosyltransferase activities in human liver microsomes and recombinant UGT enzymes

Enzyme [a]	Incubation Conditions[a]	K_m or S_{50}	V_{max}	K_{si}	*n*	CL_{int} or CL_{max} [b]
		uM	*pmol/min/mg*	*uM*		*µl/min/mg*
UGT1A1	HLM	11 ± 0.8	820 ± 20	N.A.	2.5 ± 0.4	40
	HLM + BSA	170 ± 20	1400 ± 70	N.A.	1.8 ± 0.2	4.1
	rUGT	13 ± 0.8	1300 ± 20	N.A.	2.6 ± 0.3	51
	rUGT + BSA	120 ± 4	1700 ± 30	N.A.	2.7 ± 0.2	7.6
UGT1A4	HLM	42 ± 10	1500 ± 300	64 ± 20	N.A.	36
	HLM + BSA	67 ± 10	870 ± 50	NA	N.A.	13
	rUGT	15 ± 4	970 ± 200	82 ± 30	N.A.	67
	rUGT + BSA	140 ± 60	5900 ± 2000	490 ± 300	N.A.	43
UGT1A6	HLM	420 ± 50	66000 ± 3000	15000 ± 3000	N.A.	160
	HLM + BSA	330 ± 30	47000 ± 1100	41000 ± 9000	N.A.	140
	rUGT	570 ± 50	4900 ± 200	13000 ± 2000	N.A.	8.6
	rUGT + BSA	490 ± 200	5400 ± 1000	17000 ± 10000	N.A.	11
UGT1A9	HLM	98 ± 30	1400 ± 300	690 ± 200	N.A.	14
	HLM + BSA	46 ± 4	780 ± 10	N.A.	N.A.	17
	rUGT	200 ± 70	2000 ± 500	330 ± 100	N.A.	10
	rUGT + BSA	63 ± 10	1300 ± 90	3200 ± 1000	N.A.	20
UGT2B7	HLM	610 ± 30	2100 ± 30	N.A.	N.A.	3.5
	HLM + BSA	150 ± 10	4700 ± 50	N.A.	N.A.	32
	rUGT	900 ± 30	900 ± 10	N.A.	N.A.	1.1
	rUGT + BSA	320 ± 10	3100 ± 40	N.A.	N.A.	9.8

K_m, apparent substrate concentration at half-maximal velocity; S_{50} apparent substrate concentration at half-maximal velocity for substrates exhibiting atypical kinetics; V_{max}, maximal velocity; K_{si}, inhibition constant for substrates exhibiting substrate inhibition kinetics; *n*, Hill coefficient; CL_{int}, intrinsic clearance; CL_{max}, maximal clearance; N.A., not applicable.

[a] HLMs or rUGTs (0.025 mg/ml) were fully activated with alamethicin (10 µg/ml) and incubated with increasing substrate concentrations in 100 mM Tris-HCl buffer (pH = 7.5) containing $MgCl_2$ (5 mM), UDPGA (5 mM), with or without 2% BSA as described under *Materials and Methods.* Values were not corrected for nonspecific binding in incubation and represent mean ± S.E.M. for three to four experiments.

[b] $CL_{int,}$ applies to all UGTs except UGT1A1 where $CL_{max,}$ was calculated since ES3-G formation displays atypical kinetics as described under *Materials and Methods.*

TABLE 4. Unbound kinetic parameters for human UDP-glucuronosyltransferase activities in human liver microsomes

Enzyme [a]	Incubation Conditions[a]	$f_{u,inc}$	$K_{m,u}$ or $S_{50,u}$	V_{max}	$K_{si,u}$	$CL_{int,u}$ or $CL_{max,u}$ [b]
			uM	*pmol/min/mg*	*uM*	*µl/min/mg*
UGT1A1	HLM	0.14	1.4	820	N.A.	290
	HLM + BSA	0.039	6.6	1400	N.A.	110
UGT1A4	HLM	0.28	11	1500	18	130
	HLM + BSA	0.061	4.1	870	N.A.	210
UGT1A6	HLM	0.93	390	66000	14000	170
	HLM + BSA	0.90	300	47000	37000	160
UGT1A9	HLM	1.0	98	1400	690	14
	HLM + BSA	0.17	7.8	780	N.A.	100
UGT2B7	HLM	0.69	420	2100	N.A.	5.1
	HLM + BSA	0.69	100	4700	N.A.	47

$f_{u,inc}$, mean unbound fraction in incubation determined at substrate concentrations close to K_m or S_{50} for ES (170 µM), TFP (67 µM), AZT (373 µM), or a concentration range for 5HTOL (3, 30, 300 µM) and PRO (4, 40 µM); $K_{m,u}$, unbound apparent substrate concentration at half-maximal velocity; $S_{50,u}$, unbound apparent substrate concentration at half-maximal velocity for substrates exhibiting atypical kinetics; V_{max}, maximal velocity; $K_{si,u}$, unbound inhibition constant for substrates exhibiting substrate inhibition kinetics; $CL_{int,u}$, unbound intrinsic clearance; $CL_{max,u}$, unbound maximal clearance; N.A., not applicable.

[a] HLMs or rUGTs (0.025 mg/ml) were fully activated with alamethicin (10 µg/ml) and incubated with increasing substrate concentrations in 100 mM Tris-HCl buffer (pH = 7.5) containing $MgCl_2$ (5 mM), UDPGA (5 mM), with or without 2% BSA as described under *Materials and Methods.* Values represent mean ± S.E.M. for three to four experiments.

[b] $CL_{int,u}$ applies to all UGTs except UGT1A1 where $CL_{max,u}$ was calculated since ES3-G formation displays atypical kinetics as described under *Materials and Methods.*

TABLE 5. Inhibition of human UDP-glucuronosyltransferase activities in recombinant UGT enzymes

Inhibitor	Percent activity remaining									
	rUGT1A1		rUGT1A4		rUGT1A6		rUGT1A9		rUGT2B7	
	50 μM	*500 μM*	*50 μM*	*500 μM*	*50 μM*	*500 μM*	*50 μM*	*500 μM*	*50 μM*	*500 μM*
UGT Inhibitors										
Chrysin	2	2	60	14	56	41	37	21	35	55
Diflunisal	62	9	103	96	90	20	13	2	96	68
Mefenamic acid	63	10	89	53	76	32	3	2	7	1
Silybinin	6	1	22	6	100	48	126	1	74	16
Tangeretin	14	25	71	64	22	69	6	5	76	55
Valproic acid	97	104	107	107	100	89	94	70	92	83
Cytochrome P450 Inhibitors										
1-Aminobenzotriazole	102	102	99	98	100	100	99	80	124	111
Itraconazole	11	6	13	10	89	85	84	58	91	87
Ketoconazole	17	1	15	3	80	86	110	10	12	0
Ritonavir	18	4	5	1	100	100	73	44	64	46
Verapamil	35	9	72	39	63	43	70	16	79	22

Recombinant UGTs (0.025 mg/ml) were incubated with alamethicin (10 µg/ml), 50 µM or 500 µM inhibitor (or DMSO solvent control) in 100 mM Tris-HCl buffer (pH = 7.5) containing $MgCl_2$ (5 mM), UDPGA (5 mM), without 2% BSA as described under *Materials and Methods*. Percent activity remaining (relative to solvent control) represent the mean of two experiments.

UGT substrate concentrations were at or below the respective K_m; ES (10 µM), TFP (10 µM), 5HTOL (350 µM), PRO (200 µM), AZT (842 µM).

TABLE 6. Inhibition of human UDP-glucuronosyltransferase activities in human liver microsomes and recombinant UGT enzymes

Inhibitor and Incubation Conditions [a]	IC_{50} [b]				
	UGT1A1	UGT1A4	UGT1A6	UGT1A9	UGT2B7
			μM		
Chrysin					
HLM	4.6	38	>100 [c,d]	43	15
HLM + BSA	24	>100 [c]	>100 [c]	26	>100 [c]
rUGT	6.1	43	22	>100 [c]	23
rUGT + BSA	13	>100 [c]	>100 [c]	>100 [c]	>100 [c]
Itraconazole					
HLM	0.42	0.97	>100 [c]	>100 [c]	>100 [c]
HLM + BSA	1.5	0.71	>100 [c]	>100 [c]	>100 [c]
rUGT	36	0.70	>100 [c]	>100 [c]	>100 [c]
rUGT + BSA	>100 [c]	1.06	>100 [c]	>100 [c]	>100 [c]

[a] HLMs or rUGT (0.025 mg/ml) were fully activated with alamethicin (10 μg/ml) and incubated with increasing inhibitor concentrations (0.1-100 μM) in 100 mM Tris-HCl (pH = 7.5) buffer containing $MgCl_2$ (5 mM), UDPGA (5 mM), with or without 2% BSA as described under *Materials and Methods.* UGT substrate concentrations were at or below K_m; ES (10 μM or 100 μM with BSA), TFP (40 μM HLM or 67 μM with

BSA; 10 μM rUGT or 140 μM with BSA), 5HTOL (350 μM), PRO (100 μM HLM, 200 μM rUGT, or 40 μM with BSA), AZT (842 μM HLM, 1080 μM rUGT, 374 μM HLM with BSA, or 596 μM rUGT with BSA).

[b] IC_{50} values represent mean from two experiments and are not corrected for nonspecific binding.

[c] Negligible or low degree of inhibition (IC_{50} > 100 μM).

[d] Low degree of inhibition, 40% activity remaining at 100 μM chrysin.

Figure 1

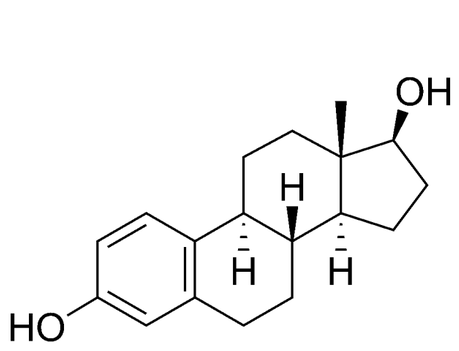

β-Estradiol

UGT1A1

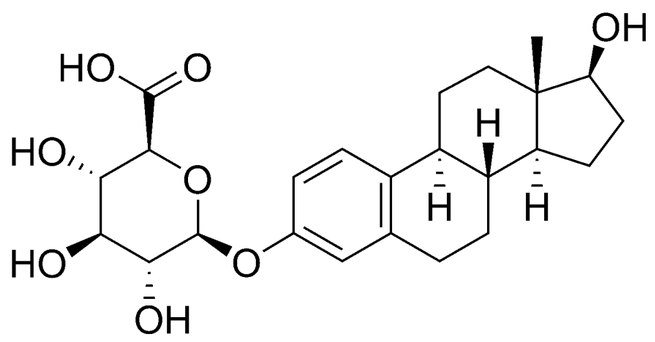

β-Estradiol-3-Glucuronide

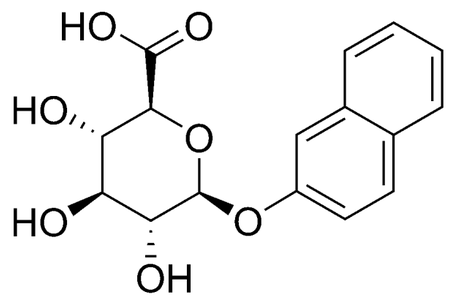

1-Naphtyl-Glucuronide

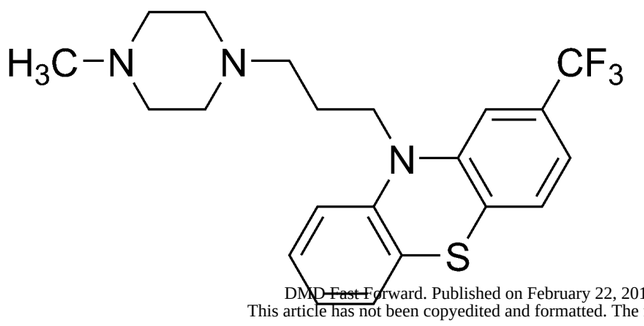

Trifluoperazine

UGT1A4

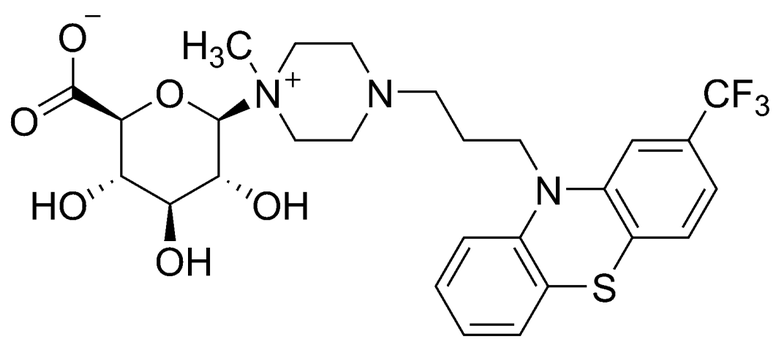

Trifluoperazine-*N*-Glucuronide

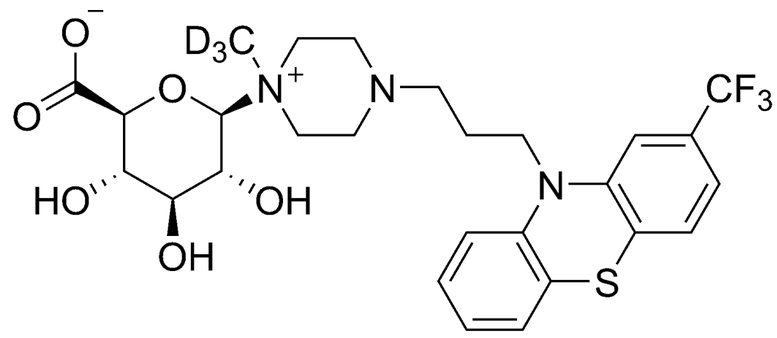

[D_3]Trifluoperazine-*N*-Glucuronide

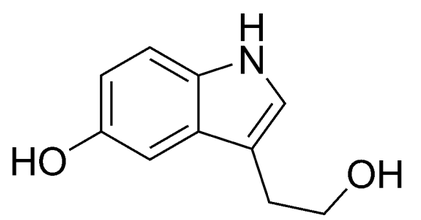

5-Hydroxytryptophol

UGT1A6

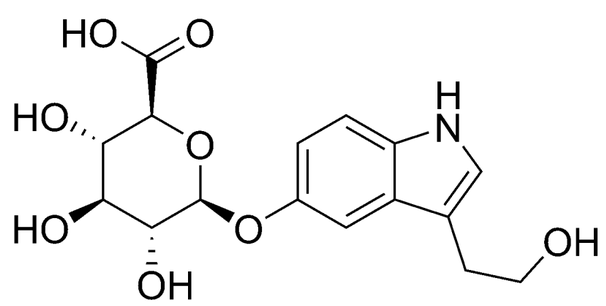

5HTOL-*O*-Glucuronide

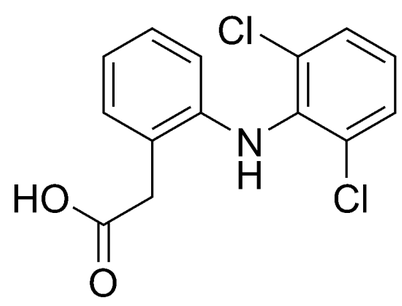

Diclofenac

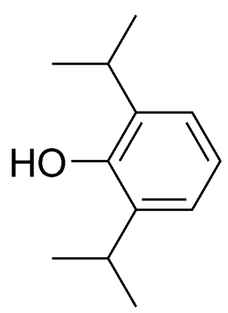

Propofol

UGT1A9

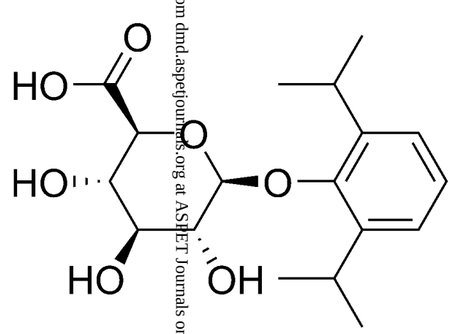

Propofol-*O*-Glucuronide

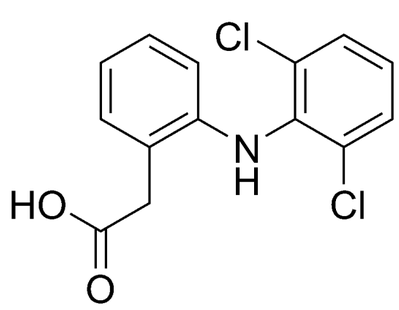

Diclofenac

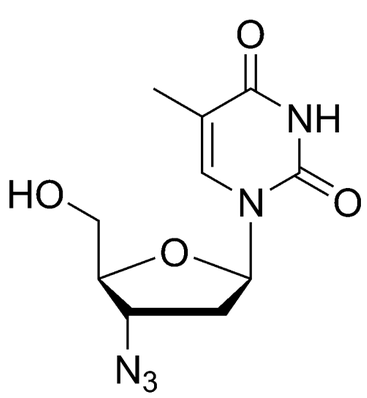

Zidovudine (AZT)

UGT2B7

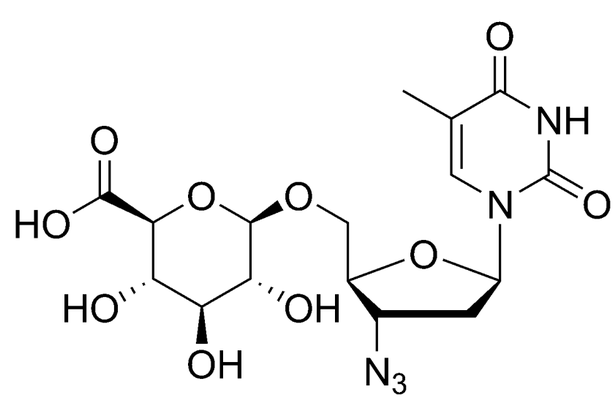

AZT-5'-Glucuronide

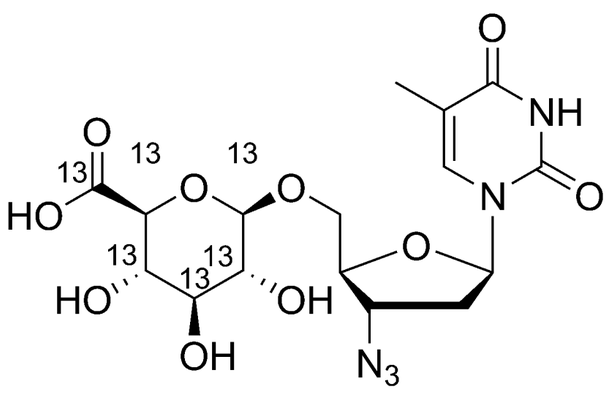

[$^{13}C_6$]AZT-5'-Glucuronide

DMD Fast Forward. Published on February 22, 2012 as DOI: 10.1124/dmd.111.043117
This article has not been copyedited and formatted. The final version may differ from this version.

Figure 2

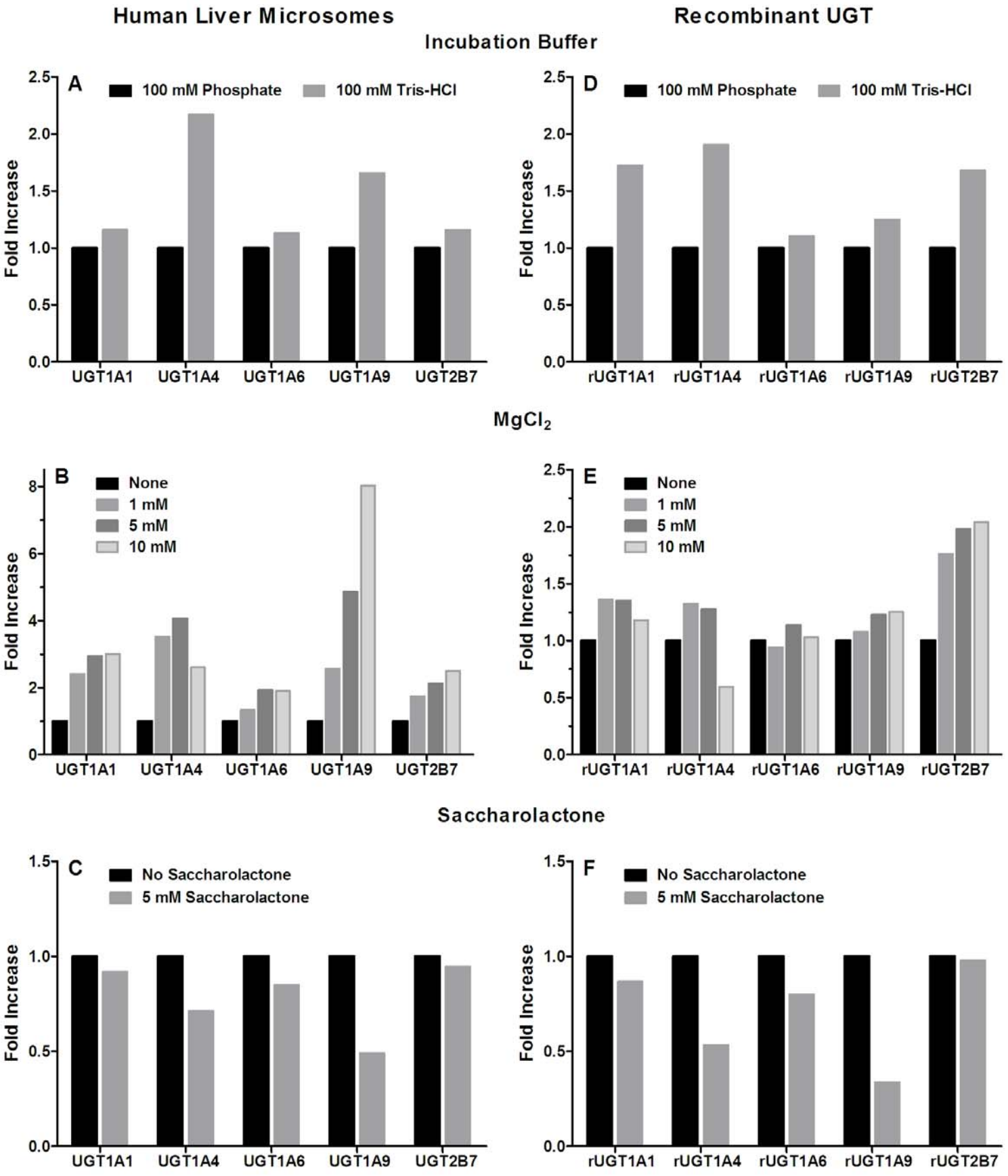

Figure 3

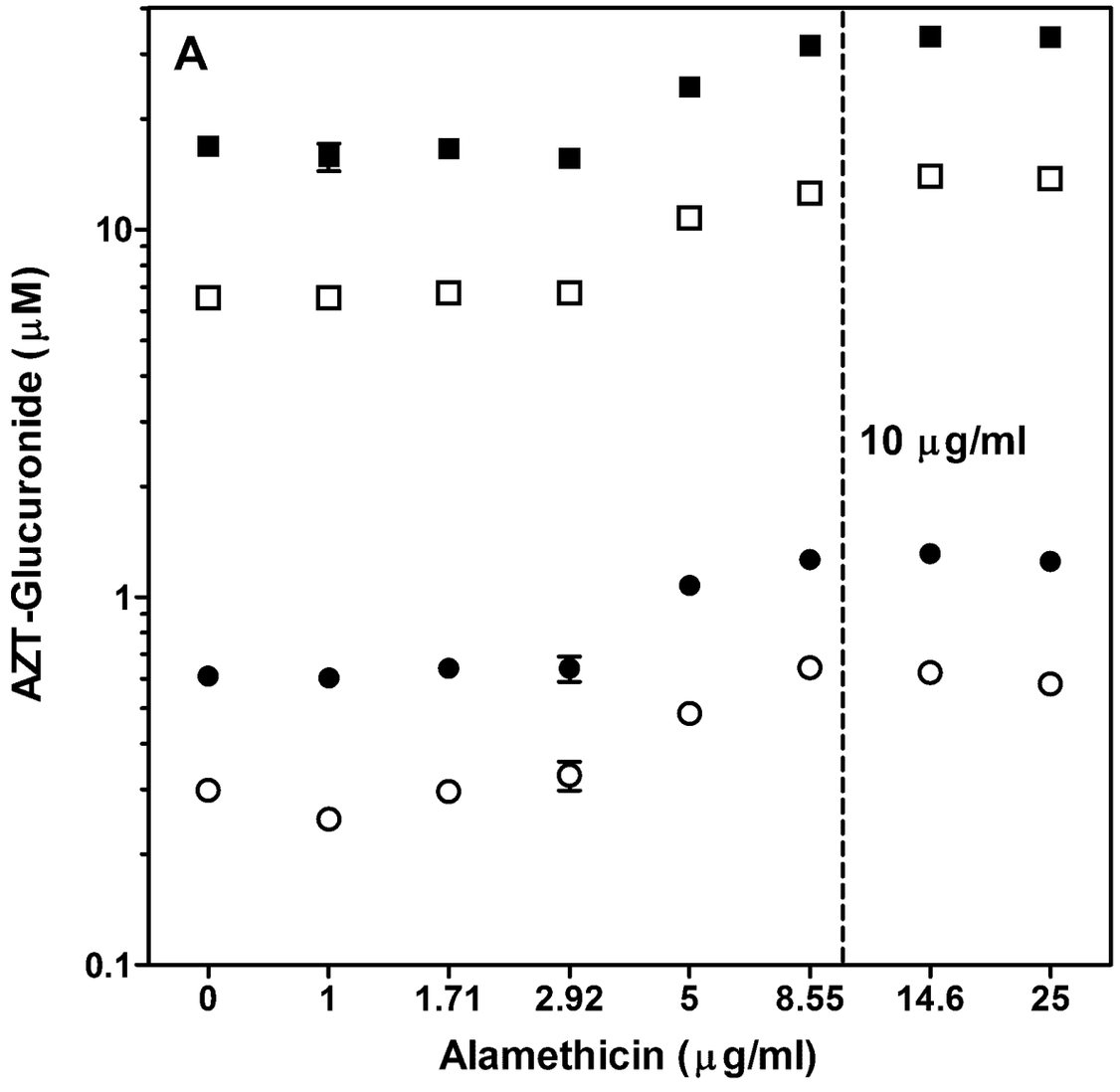

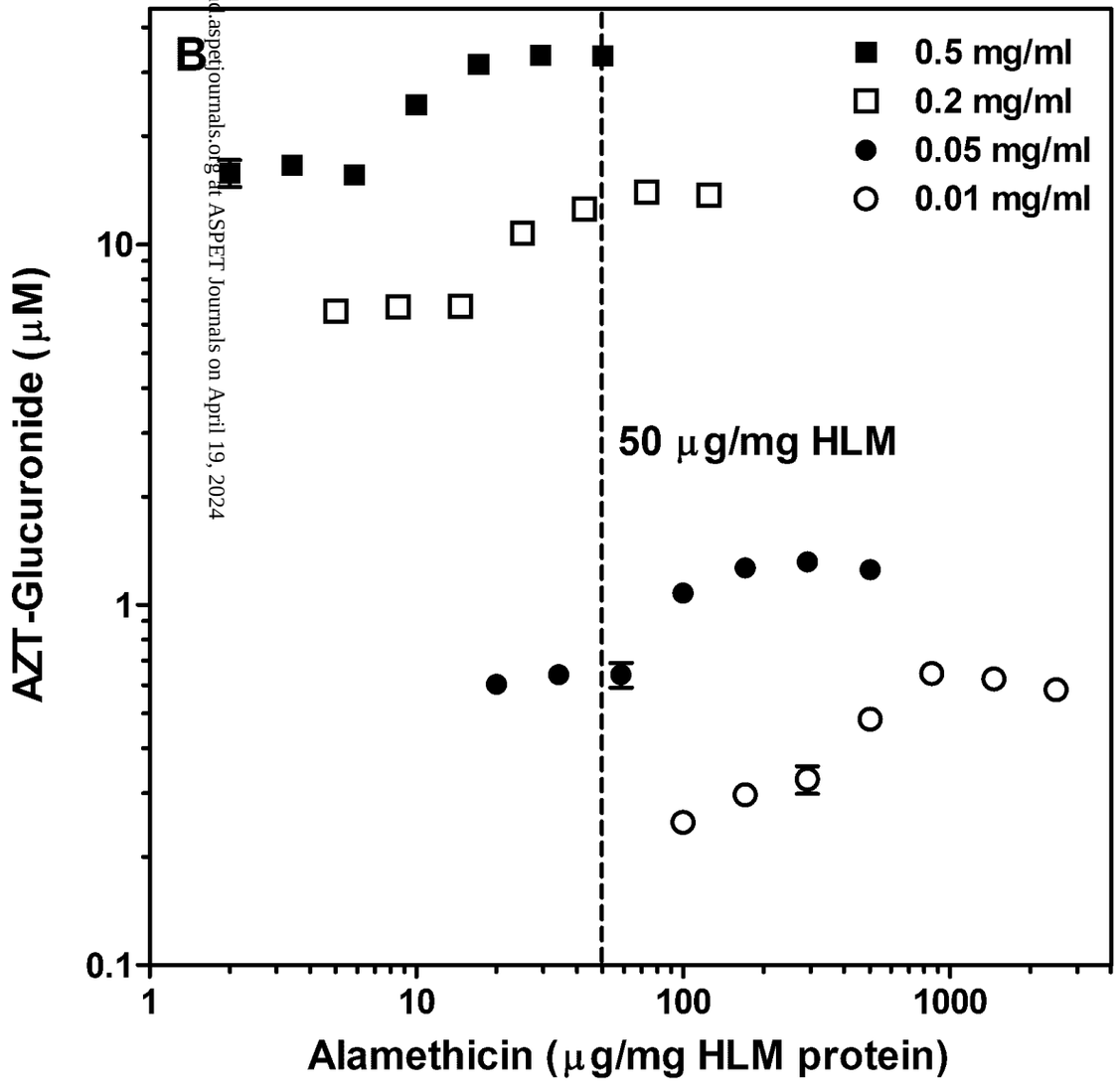

Figure 4

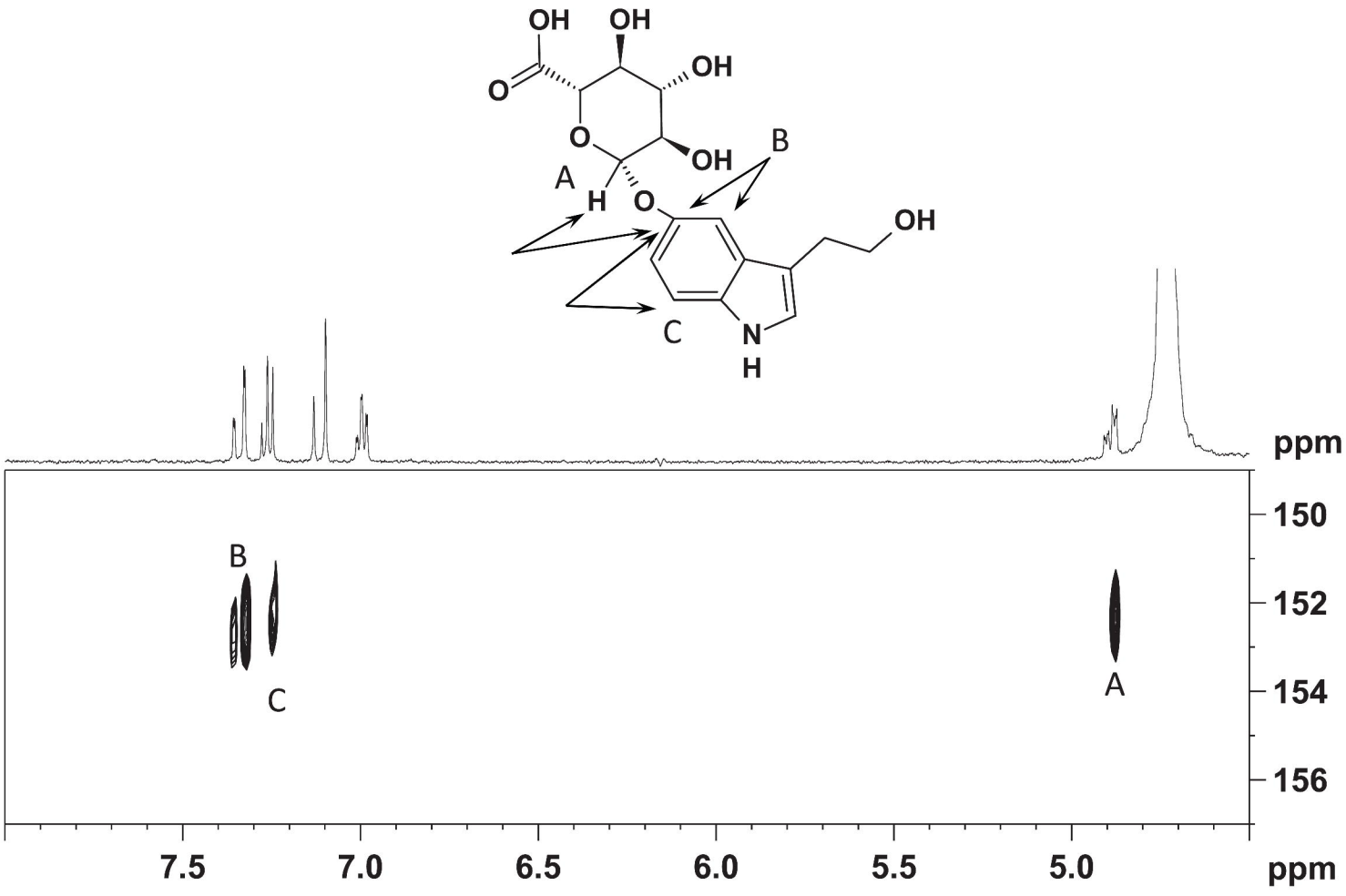

Figure 5

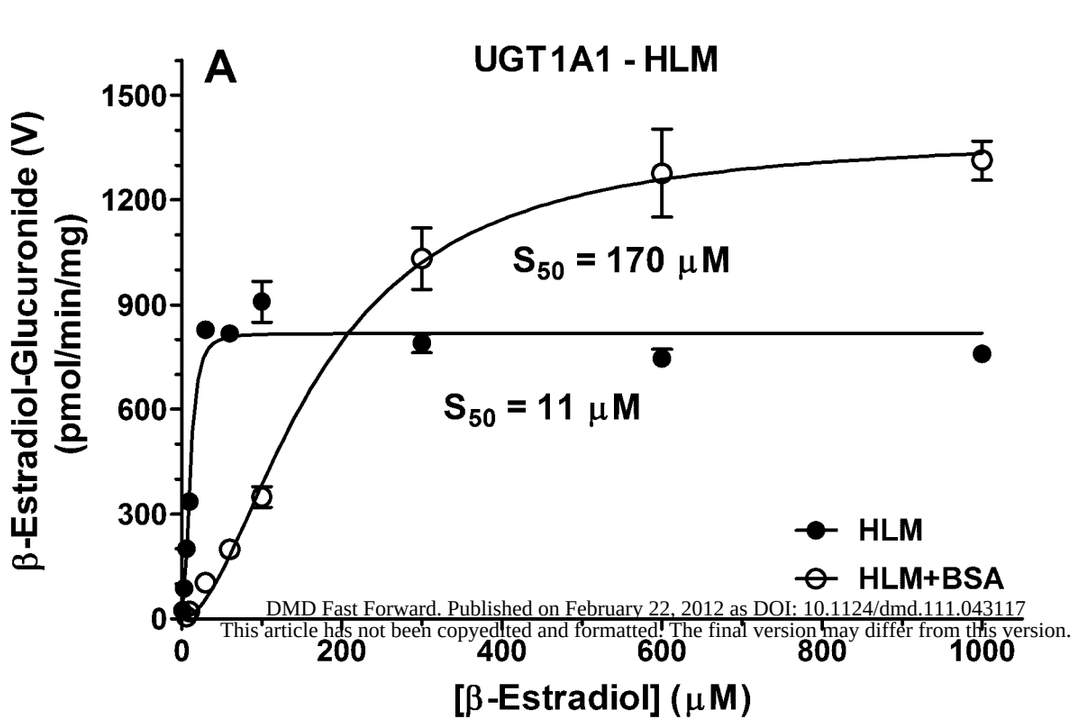

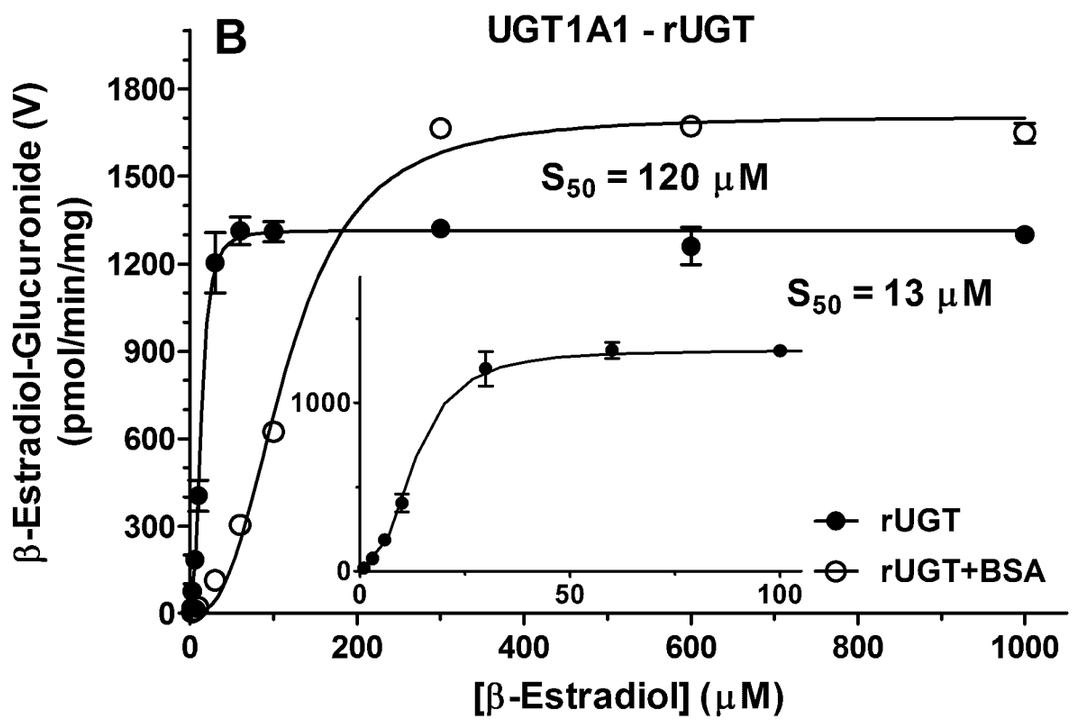

DMD Fast Forward. Published on February 22, 2012 as DOI: 10.1124/dmd.111.043117
This article has not been copyedited and formatted. The final version may differ from this version.

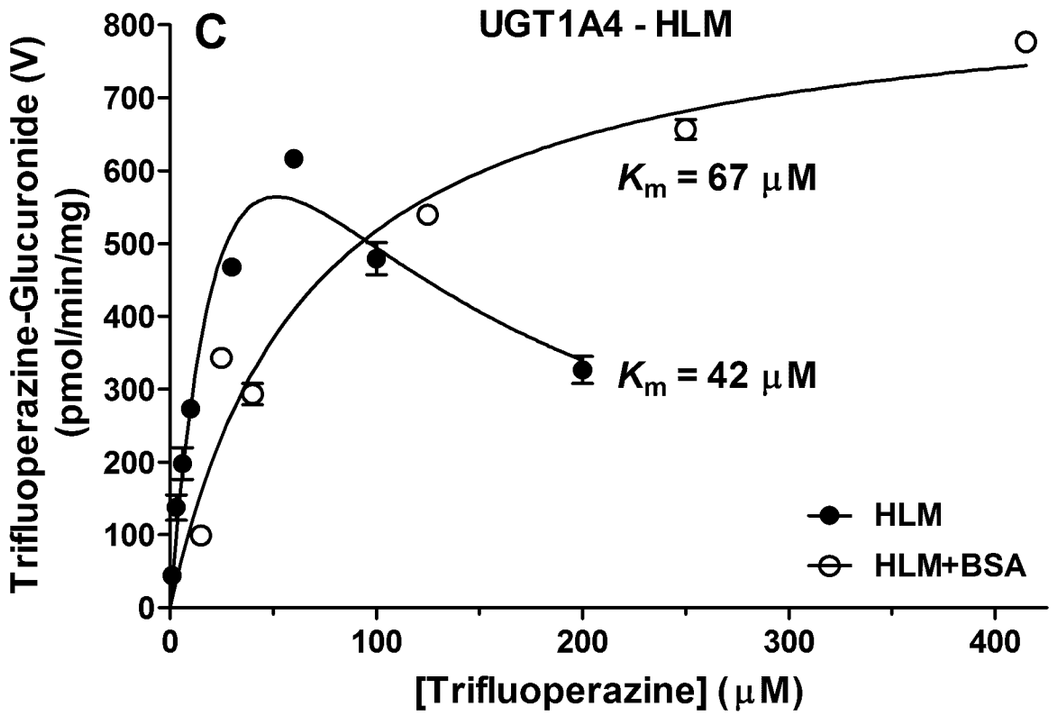

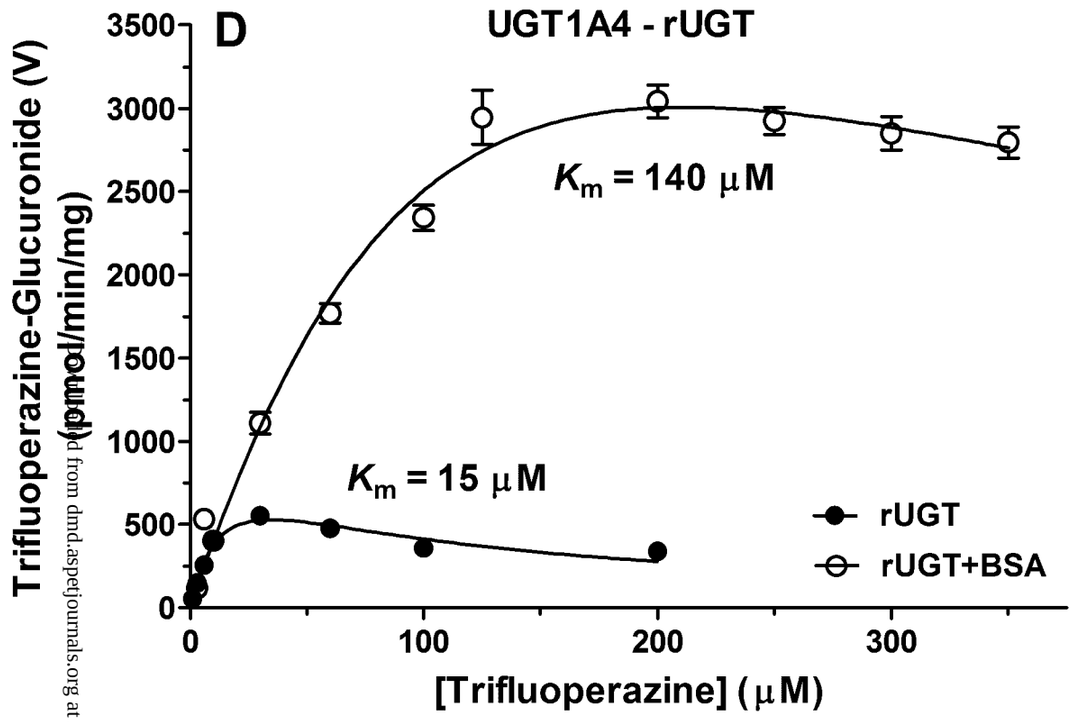

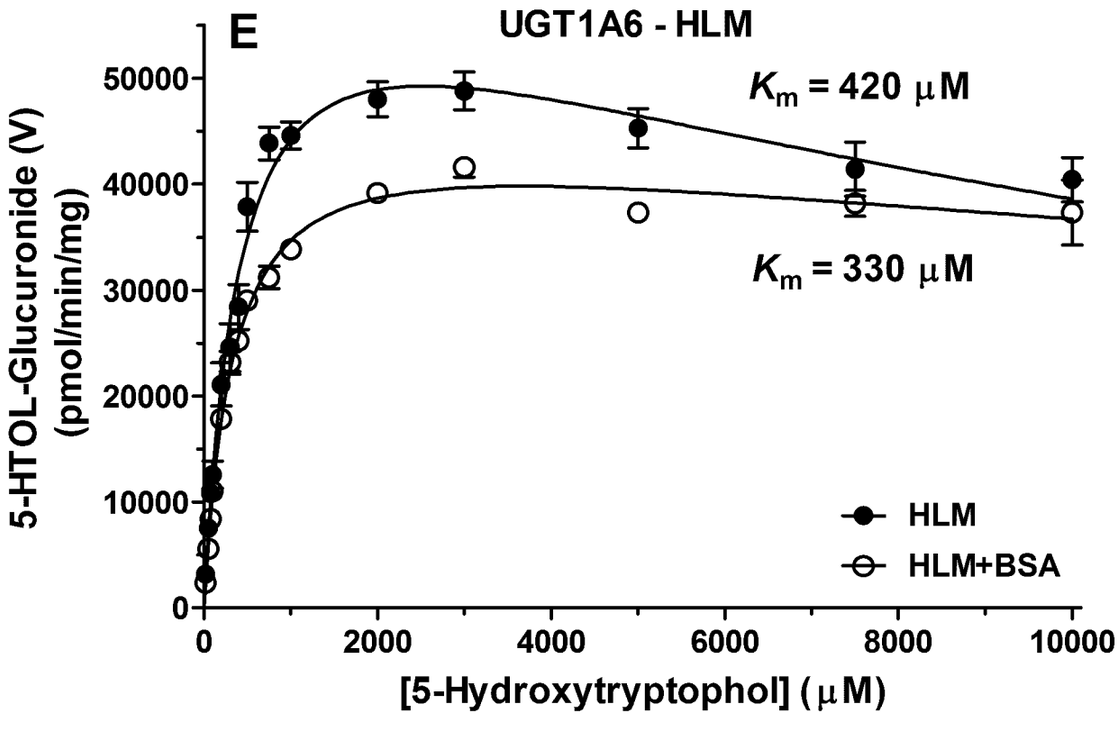

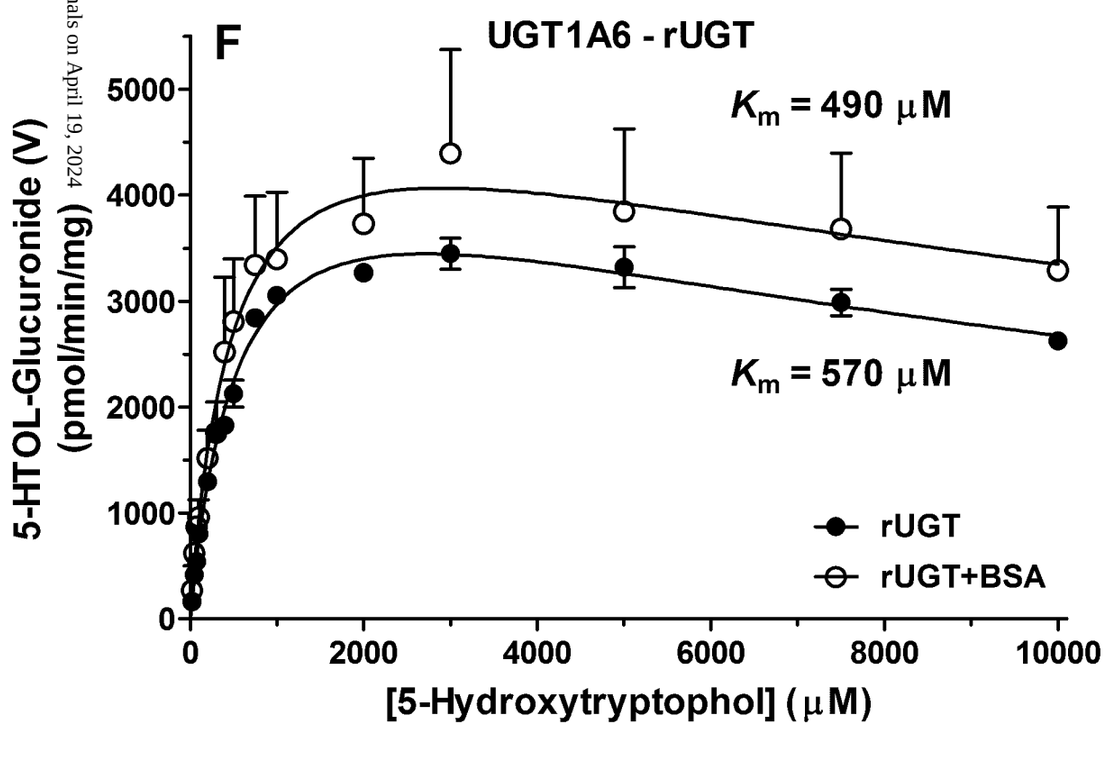

Figure 6